SOIL VOLCANIC ASH AND DOUGLAS-FIR (*Pseudotsuga menziesii* [Mirb.] Franco var. *glauca*) PRODUCTIVITY IN NORTH CENTRAL IDAHO

A Dissertation

Presented in Partial Fulfillment of the Requirements for the

Degree of Doctor of Philosophy

with a

Major in Natural Resources

in the

College of Graduate Studies

University of Idaho

By

Mark James Kimsey, Jr.

May 2006

Major Professor: James A. Moore, Ph.D.

AUTHORIZATION TO SUBMIT

DISSERTATION

This dissertation of Mark James Kimsey, Jr., submitted for the degree of Doctor of Philosophy with a major in Natural Resources and titled "Soil Volcanic Ash and Douglas-Fir (*Pseudotsuga menziesii* [Mirb.] Franco var. *glauca*) Productivity in North Central Idaho," has been reviewed in final form. Permission, as indicated by the signatures and dates given below, is now granted to submit final copies to the College of Graduate Studies for approval.

Major Professor_____ Date _____
James A. Moore

Committee Members _____ Date _____
Leonard R. Johnson

_____ Date _____
Paul E. Gessler

_____ Date _____
Paul A. McDaniel

_____ Date _____
Daniel L. Miller

_____ Date _____
Dean Stuck

Department Administrator_____ Date _____
Jo Ellen Force

College Dean _____ Date _____
Steven B. Daley-Laursen

Final Approval and Acceptance by the College of Graduate Studies

_____ Date _____
Margrit von Braun

ABSTRACT

Volcanic ash distribution, thickness, and its role in Douglas-fir (*Pseudotsuga menziesii* [Mirb.] Franco var. *glauca*) site index (SI) were determined for a forested region of north central Idaho. Ash thickness (AT) and Douglas-fir SI measurements were collected from local Natural Resource Conservation Service soil surveys and through newly installed field plots. Climatic, ecological, edaphic, geologic, and topographic data were collected from field observations or derived from digital elevation models. Three statistical models were developed to estimate AT and two models for predicting Douglas-fir SI. The modelled relationships were spatially displayed using a geographicl information system (GIS).

Statistical model 1 was developed to estimate AT using ecologically based plant associations as an explanatory variable. Climax plant associations moister than grand fir-queen cup beadlily (*Abies grandis*/*Clintonia uniflora*) had consistently thick ash mantles and soils that would be classified as either Andisols or andic subgroups using Soil Taxonomy. Multiple linear regression (MLR) results showed that topographic factors accounted for ~ 29 percent of the explained variance, with elevation accounting for ~ 18 percent alone. Plant associations accounted for ~ 71 percent of the explained variation in AT. The statistical model error of 10.7 cm was significantly lower than the >20 cm variation often found in local soil series. Overall model fit produced an R^2 of 0.6. Results suggest that plant associations integrate many of the local factors that influence volcanic ash distribution.

Statistical model 2 was developed to determine AT for situations when climax plant associations are not physically observable. This model was based solely upon topographic factors. Predictive models were developed using MLR and geographically weighted regression (GWR). Results show that elevation, slope, plan curvature, and the wetness index

all significantly influence volcanic ash distribution. Similar to model 1, elevation explained the most variation in AT. GWR improved model fit and precision by 36 percent and 30 percent, respectively, over the MLR model (R^2_A = 0.64). The localized approach of GWR modelling showed that elevation, slope curvature, and the wetness index behaved differently depending on geographic location. This suggests that the global approach of MLR modelling is masking conditional landscape relationships that are unique and highly localized.

Volcanic ash and other climatic, edaphic, geologic, and topographic factors were used to predict Douglas-fir SI using both MLR and GWR in statistical model 3. Elevation, ash depth, slope, and aspect were significantly correlated with Douglas-fir SI. Elevation was found to be nonstationary, indicating that parameter estimates associated with elevation significantly change depending on the geographic location of an observation. SI showed a positive logarithmic response to increasing AT. GWR significantly improved MLR model fit by 28 percent and reduced the sum of square errors by 54 percent (R^2_A = 0.5). Residuals analysis of MLR SI estimates showed extreme SI overestimation in the south and west portion of our study area. This overestimation was significantly reduced in the GWR model. The significant fit and precision improvements of GWR models suggest that the complex interactions affecting Douglas-fir SI are better analyzed at the local level.

ACKNOWLEDGEMENTS

With much gratefulness I wish to thank Dr. Jim Moore for 11 years of mentoring at the undergraduate and graduate level. Dr. Moore's support through these many years is humbling and deeply cherished. I also wish to thank my graduate committee, Drs. Leonard Johnson, Paul Gessler, Paul McDaniel, Dean Stuck, and Dan Miller for their support and assistance during this project.

Special acknowledgement and appreciation is due Potlatch Corporation for their financial and clerical assistance in this project. The support of Dr. Dean Stuck in obtaining funding for this project is especially appreciated. I would like to thank Dr. Dan Miller and Rob Taylor for their assistance in the many aspects of this research project. Also, I wish to thank the Potlatch Research Committee for their continued interest in my project. Intermountain Forest Tree Nutrition Cooperative personnel Dr. Leonard Johnson, Terry Shaw, Peter Mika, and Dr. Mariann Garrison-Johnston provided valuable assistance during this project. Their technical expertise and personal support provided many academic and personal growth opportunities. Natural Resource Conservation Service Staff Brian Gardner, Eileen Rowan, and Frank Gariglio are gratefully acknowledged for their expert advice and assistance in this project.

I wish to thank Grandma Wheaton, Cousin Andi "Bear" Ruffing, Mrs. Woolston, Adams, Sandbergs, and the many friends and family who have participated in my life through prayer and friendship. Your participation is deeply treasured. To my Dad, Mom, and Brother, I owe you all. Words cannot express my heartfelt gratitude for the personal, spiritual, and financial support you have poured into me over the many years. To all: "The Lord bless thee, and keep thee: The Lord make his face shine upon thee, and be gracious unto thee: The Lord lift up his countenance upon thee, and give thee peace" (Num. 6:24-26).

DEDICATION

To my Lord and Saviour, Jesus Christ.

Thank you for providing me with family and mentors who have poured their lives into me,

as you poured out your life for all.

TABLE OF CONTENTS

CHAPTER 3: A geographically weighted regression analysis of Douglas-fir (*Pseudotsuga menziesii* [Mirb.] Franco var. *glauca*) site index in north central Idaho.

LIST OF FIGURES

LIST OF TABLES

INTRODUCTION

Volcanic ash distribution and its potential effect on Douglas-fir (*Pseudotsuga menziesii* [Mirb.] Franco var. *glauca*) site index (SI) was modelled for a north central Idaho forest located in the Natural Resource Conservation Service (NRCS) ID-612 soil survey area. This area was selected for study based upon the large number of soil and timber productivity records available. Previous Douglas-fir SI studies within the Inland Northwest have shown either minimal or inconclusive effects of volcanic ash on tree height. Many of these studies were based on small datasets covering large geographic regions that ultimately confounded edaphic, climatic, and topographic variables. Another goal of our study was to provide a quantitative assessment of regional volcanic ash distribution. Statistical analyses of the ID-612 soil survey data were conducted in an effort to determine if a large dataset of soil and timber productivity records within a small geographic area could provide more precise models for determining volcanic ash distribution and ultimately, Douglas-fir SI. Developed models were then spatially evaluated within a geographic information system (GIS).

The presence of volcanic ash is often associated with moist plant communities and moisture accumulating landscape positions within the Inland Northwest. These associations are variable across the region, and have never been quantified locally. Rough approximations of ash thickness (AT) can be determined through local soil survey units, but they provide only a range of potential thicknesses. In Chapter 1 of this dissertation, ash distribution and thickness were assessed using plant associations and topographic variables. Comparative analyses of mean AT by classed variable were performed. Environmental variables were used to model AT using multiple linear regression (MLR). Model fit and precision statistics

were obtained to determine the model's usefulness for estimating volcanic AT within north central Idaho.

Reliance on plant associations to derive ash distribution patterns may not always be an option. Management activities, biological predation, wildfire, or climate change often shift plant associations away from climax. These scenarios could confound a model that is reliant on the physical site expression of climax plant associations. In Chapter 2, volcanic ash distribution is modelled solely with topographic features. Topographic features were derived from a United States Geological Survey (USGS) 30-m digital elevation model (DEM) and were modelled using MLR and geographically weighted regression (GWR). GWR was conducted to assess the potential nonstationary effects of topography on AT, and to provide a local alternative to ordinary MLR modelling. The two statistical models were compared to determine the effectiveness of localized regression modelling in capturing additional sources of variation. Model results were then spatially displayed in a geographic information system (GIS).

Chapter 3 shifts the focus from volcanic ash to Douglas-fir SI modelling. The effects of edaphic, geologic, topographic, and climatic factors on Douglas-fir SI were evaluated. SI models were derived from these environmental variables using MLR and GWR. Statistical techniques used in Chapter 2 were applied to SI modelling. Model estimates and residuals were spatially displayed to show the strengths and weaknesses of the two models. The GWR approach performed well for estimating SI, and highlighted the potential consequences of assuming independent variable stationarity when it does not exist.

The goal and findings of this study is to provide forestland managers with important information on the distribution of volcanic ash and its effect on Douglas-fir SI within north

central Idaho. Statistical models developed within this study can be used in natural resource management prescriptions and applications. In addition, spatial maps have the potential to aid decision support systems and particularly enhance the selection of land based harvest systems (minimizing ash disturbance) and potential areas for fertilizer applications (increasing return on investment in more productive areas).

CHAPTER 1: Ecological and Topographic Features of Volcanic Ash-Influenced Forest Soils

ABSTRACT

Volcanic ash distribution and thickness were determined for a forested region of north central Idaho. Mean ash thickness (AT) and multiple linear regression (MLR) analyses were used to model the effect of environmental variables on AT. Slope and slope curvature relationships with AT varied on a local spatial scale across the study area. AT and aspect showed weak correlation. Elevation and ecologically based plant associations accounted for about 54 percent of the observed variation in AT. Climax plant associations moister than grand fir-queen cup beadlily (*Abies grandis*/*Clintonia uniflora*) had consistently thick ash mantles and soils that would be classified as either Andisols or andic subgroups using Soil Taxonomy. The statistical model error of 10.7 cm was significantly lower than the >20 cm variation often found in local soil series. This model quantitatively assesses AT and can be integrated into other local ecological models.

INTRODUCTION

Volcanic ash from eruptions along the Pacific Northwest Cascade Range has significantly influenced forest soils of the Inland Northwest, USA (Mullineaux, 1986; Shipley and Sarna-Wojcicki, 1983). The Holocene era eruption of Mt. Mazama (now Crater Lake, OR) distributed >116 km^3 of volcanic tephra across this region (Bacon, 1983; Zdanowicz et al., 1999). Soils influenced by the deposition of Mt. Mazama tephra can be found throughout the western United States and into southwestern Canada (Figure 1.1). Soils formed in, or influenced by volcanic ash are important to forest management. Volcanic ash-influenced soils have lower bulk density, higher porosity, and higher water infiltration and retention than soils less influenced or unaffected by ash (McDaniel et al., 2005; Nanzyo et al., 1993; Nimlos, 1980; Warkentin and Maeda, 1980). Among the benefits of these soil properties is the reduction in drought stress on plant communities during extended summer dry periods.

Deposition of Mt. Mazama ash in the Columbia basin of eastern Washington State was estimated at approximately 15-20 cm thick, with thinning in areas more distal to the eruption (Busacca et al., 2001). The current distribution pattern of volcanic glass derived from the Mazama event is much different than this original deposition pattern. Busacca et al. (2001) found only weak tephra influence in soils of the southwest Columbia Plateau even though these areas are closest to the volcanic source of the tephra. Instead, glass content of the surface soils increases with increasing downwind distance from the source volcano.

Several mechanisms have been proposed as factors in the transformation of the original tephra sheet into the current mixed distribution patterns. Busacca et al. (2001) submit that extensive re-working of volcanic ash by wind occurred during the mid-Holocene drought (7,600 – 5,000 yr BP). Prevailing southwesterly wind patterns re-entrained unincorporated

Figure 1.1. Estimated spatial distribution of Mt. Mazama volcanic ash across the western United States and southwestern Canada. The study area for this research project is located within the boxed area of north central Idaho (adapted from Williams and Goles, 1968).

volcanic ash and transported it downwind. This process of re-entrainment and re-deposition is enhanced by the physical characteristics of Mt. Mazama ash. Regional volcanic ash is characterized by low cohesiveness and a high percentage of silt-sized particles. These properties readily produce a soil that is susceptible to wind erosion when dry (Dubroeucq et al., 1998). Several additional mechanisms include: 1) burial of ash by episodic loess deposition and subsequent bioturbation by soil fauna, and 2) enhanced retention and capture under moist plant communities (Busacca et al., 2001; Hunter, 1988; McDaniel et al., 2005; Nimlos and Zuuring, 1982; Zobel and Antos, 1991). Such mechanisms may explain the extensive mixing often observed in ash surface layers found in mountainous regions of the Inland Northwest.

Nimlos and Zuuring (1982) suggest that precipitation and volcanic ash distribution is positively correlated in forested regions of western Montana. Volcanic ash in the atmosphere would be transmitted to the ground during rain and snow events. Higher elevations would accumulate greater concentrations of ash as air masses cooled and released precipitation. Nimlos (1980) observed that ash in western Montana does not occur in areas with precipitation less than 560 mm. On sites with annual precipitation ranging from 560 – 1000 mm, ash is typically found on gentle or north-facing slopes, but not on very steep or southerly facing slopes. Locations that receive >1000 mm of annual rainfall exhibit ash soils on all landforms and slopes. Nimlos (1980) also suggested that the absence of volcanic ash at the base of south slopes <1000 m in elevation is attributable to wind action. Overland water movement would have redistributed the ash from shoulder and backslope to the foot and toeslope positions. Lack of ash in these slope positions suggests that wind, not water, was the primary eroding factor (Nimlos, 1980).

Nimlos and Zuuring (1982) also attempted to predict ash distribution and thickness as a function of habitat type and terrain attributes. Their rationale for including forest vegetation habitat types was related to the relatively high water holding capacity of volcanic ash. Soils influenced by volcanic ash will have wetter soil moisture regimes (SMR) than those soils not influenced by volcanic ash. Consequently, moister SMR's will shift plant communities toward climax (Barker, 1981; Cooper et al., 1991; Steele et al., 1981). It follows that thicker volcanic ash mantles would hold more water and thus support successively moister plant communities. However, Nimlos and Zuuring (1982) were unable to uncover any strong statistical correlation between habitat type and volcanic ash thickness. Additionally, terrain attributes and their transformations and interactions, could not reliably predict volcanic ash thickness. A potential explanation for poor model performance was a data gap in ash thickness ranges. Within their dataset, only 7 observations had ash mantles <10 cm and none were <8 cm. This lack of heterogeneity in observed ash thickness suggests that environmental variables associated with minimal ash influence were not accounted for in their model.

Recent Natural Resource Conservation Service (NRCS) soil surveys have extensively mapped volcanic ash-influenced forest soils in portions of the Inland Northwest. Ash distribution and ecological/topographic relationships can be assessed from these surveys; however, these soil survey relationships are often presented as a range in ash thickness. For example, volcanic ash thicknesses in Hugus and Bouldercreek soil series commonly found in our study area, have mapped variations >20 cm (Soil Survey Division, 2006). In a review of the correlation between forest soils and vegetation patterns, Hironaka et al. (1991) point out that habitat type and soil classification schemes are often fuzzy due to the level of variation

allowed in the abstract units. It is often difficult to assess whether these abstract units reflect ecological reality due to site disturbance.

As more information is gathered on the role of volcanic ash in forest productivity and management, natural resource managers may need finer resolution of ash distribution than a range in ash thickness. The inherent variation of soil surveys may not provide the level of accuracy needed for decision support systems. Absent the research of Nimlos and Zuuring (1982), few efforts to date have focused on quantitatively defining Mt. Mazama ash distribution and thickness within the Inland Northwest. This situation is partially due to the extensive diversity of landform, climate, and geographical extent of volcanic ash distribution throughout the Inland Northwest. As is evident from Nimlos and Zuuring's (1982) work in western Montana, the data available for developing fine resolution assessments of volcanic ash distribution have been too limited to cover the variation in large geographical regions.

Quantitative ash distribution assessments must therefore be conducted over smaller geographic areas. This implies that sampling designs be constructed to elucidate critical environmental variables that contribute to ash distribution variation. Once identified, these variables can be sampled to capture the inherent variation in ash thickness. A potentially workable alternative is a statistical re-analysis of individual soil-site descriptions created during local NRCS soil surveys. Data of this nature would typically need to be converted from the raw field sheets to a database, but the process would reduce the time and financial resources necessary for quantifying volcanic ash distribution patterns.

Based on the above rationale, our objective was to select a relatively small geographic region within the Inland Northwest for which extensive soil and environmental data was available to: i) develop a dataset of volcanic ash depths, habitat types, and terrain attributes;

ii) conduct statistical analyses to assess relationships between ash thickness and selected vegetative and topographic features; and iii) determine the precision and fit of a statistical model to estimate the thickness of volcanic ash across a landscape.

MATERIALS AND METHODS

Study Area

The geographic area chosen for this study is the NRCS ID-612 soil survey region located in north central Idaho (Figure 1.1). This survey area encompasses ~336,250 ha of diverse climatic factors, habitat types, and complex terrain attributes. Landscapes of this region are generally characterized as mountainous in the north and east, while the south and west are characterized as basalt plateaus/benchland incised with deep canyons. Soil parent material varies widely from metasedimentary schists and quartzites to igneous granites and basalts. Eolian deposits of loess from the Columbia Basin and volcanic ash from the eruption of Mt. Mazama are often found as intermixed mantles. Elevation ranges from 300 m in the southwest to >1700 m in the north and east. Mean annual precipitation (MAP) roughly follows the elevational gradient, with <300 mm MAP in the southwest and >1500 mm in the northeast (Idaho State Climate Services, 2000). Ponderosa pine (*Pinus ponderosa* Dougl.) and Douglas-fir (*Pseudotsuga menziesii* [Mirb.] Franco var. *glauca*) habitat types dominate the southern regions of the soil survey. Western redcedar (*Thuja plicata* Donn) and Western hemlock (*Tsuga heterophylla* [Raf.] Sarg.) dominate the warm, moist upland regions; with Subalpine fir (*Abies lasiocarpa* [Hook.] Nutt.) and Mountain hemlock (*Tsuga mertensiana* [Bong.] Carr.) predominant in the colder, higher elevations (Cooper et al. 1991).

Data Collection and Analysis

Nine hundred and twenty-one soil-site descriptions and their spatial coordinates were obtained from the Orofino, ID NRCS field office. Soil-site description locations were selected by NRCS field soil scientists to support the ID-612 soil survey. Records were collected by ~ 5 lead soil scientists over ~ 15 years. Location coordinates for the majority of the data were transcribed from aerial photos to a geographic information system (GIS). A small portion of the records was established using geographic positioning system (GPS) devices toward the end of the soil survey. For those locations obtained from aerial photos, we assumed the accuracy to be within the cell size of a United States Geological Survey (USGS) 30-m digital elevation model (DEM).

Soil-site description locations were established to capture the range in terrain and soil property characteristics established for a soil series. Each soil series was created based on landscape features that showed similar soil development. Field records composed of volcanic ash thickness, terrain attribute, and habitat type observations were entered into a database from these detailed NRCS soil-site descriptions. The effective number of observations available for analysis varied since it was not unusual for certain field observations to not be recorded on the field form. A summary of the field descriptors and their potential influence on volcanic ash distribution is presented in Table 1.1.

Soil measurements were collected from 1-m soil pits established at each location. Soil horizons were described and recorded. Terrain attributes were collected by: 1) clinometer (slope), 2) compass (aspect), and 3) topographic maps (elevation). The continuous variables elevation (ELE), slope (SLP), and aspect (ASP) were grouped into discrete classes to facilitate the comparison of incremental changes in ash thickness with terrain attributes. ELE

Table 1.1. Selected ecological and topographic features and their potential significance in determining volcanic ash distribution patterns for a forested north central Idaho landscape (Cooper et al., 1991; Wilson and Gallant, 2000).

Ecological/Topographic Features	Significance
Elevation (meters): ELE	**Climate, vegetation type, potential energy**
200-400	
400-600	
600-800	
800-1200	
1200-1400	
1400+	
Slope (%): SLP	**Overland and subsurface flow, velocity, and runoff**
0-10	
10-20	
20-30	
30-40	
40-50	
50-60	
60+	
Aspect (°): ASP	**Solar irradiation, wind erosion/deposition**
Flat	
N (342.6-27.5)	
NE (27.6-72.5)	
E (72.6-117.5)	
SE (117.6-162.5)	
S (162.6-207.5)	
SW (207.6-252.5)	
W (272.6-297.5)	
NW (297.6-342.5)	
Plan/Profile curvature: PRCU/PLCU	**Flow acceleration, erosion/deposition rate, converging/diverging flow, soil water content**
Linear	
Concave	
Convex	
Plant Associations:	**Climate, topography, site productivity, disturbance**
Vegetation Series: VS	
***Pinus ponderosa* (PIPO)**	
***Pseudotsuga menziesii* (PSME)**	
***Abies grandis* (ABGR)**	
***Thuja plicata* (THPL)**	
***Tsuga heterophylla* (TSHE)**	
***Tsuga mertensiana* (TSME)**	
***Abies lasiocarpa* (ABLA)**	
Habitat Type: HT	
***Festuca idahoensis* (FEID)**	
***Physocarpus malvaceus* (PHMA)**	
***Symphoricarpus albus* (SYAL)**	
***Linnaea borealis* (LIBO)**	
***Clintonia uniflora* (CLUN)**	
***Asarum caudatum* (ASCA)**	
***Adiantum pedatum* (ADPE)**	
***Gymnocarpium dryopteris* (GYDR)**	

was classed into 200-m intervals, SLP at 10 percent breaks, and ASP in 45-degree quadrants. Slope curvature values were derived from a USGS 30-m DEM using grid algebra in a GIS. The numerical curvature values were then grouped into their respective linear (L), concave (C), and convex (C) classes.

Average ash thickness (AT) by class was computed for each of the variables described above. Standard errors were computed and *t*-tests performed to test for significant differences in AT using an α-level of 0.1. Variables that showed significant class differences in AT were subsequently tested for use as predictor variables in a volcanic ash distribution model. Model variable measurements were assumed measured without error. This assumption was taken with caution, because of the reliance on: 1) data collected over a period of time by different field soil scientists, and 2) DEM-derived data with an accuracy of 30-m. Measurement error can lead to an inflated model error term, thus underestimating the *F*-statistic. This may lead to the elimination of variables that may have been significant if measured without error. Consequently, it cannot be assumed that insignificant independent variables have no effect on AT, because of potential observation and/or imputed error during data collection.

A stepwise variable selection procedure was used within the framework of a general linear model (GLM) to assess which categorical variables explained the greatest variation in AT. Variables that were within the upper 0.1 percentile of a Type III sums-of-squares *F*-distribution were retained within the model. The equation can be generally stated as follows:

$$AT_{(i)} = \mu + \beta_1 X_{1(i)} + \beta_2 X_{2(i)} + \ldots + \beta_k X_{n(i)} + \varepsilon_i \quad \text{[Eq. 1.1]}$$

where $AT_{(i)}$ = estimated ash thickness at observed location *i*, μ = overall ash thickness mean, $\beta_k X_{n(i)}$ = fixed effect for k^{th} independent variable at location *i*, and ε_i = model error at

location *i*. The prediction equation was deemed reliable if it produced a high coefficient of determination (R^2) and low root mean square error (RMSE).

RESULTS

Topographic and Vegetative Indicators

Volcanic ash is highly correlated with ELE (Figure 1.2). Each 200-m increment is significantly different up to 1200 m (p <0.1). Above 1200 m, there is no significant difference in mean AT. Forest soils below 600 m in elevation have ash thicknesses ≤10 cm. Many low elevation soils exhibit significant mixing of the shallow ash mantle with underlying soil material. These lower-elevation forest soils are classified as vitrandic subgroups of a soil order (Soil Survey Staff, 1999). Forest soils located at elevations between 600 m and 1200 m have mean ash thicknesses 24 to 35 cm. These soils are classified as andic subgroups. Volcanic ash mantles have a mean thickness of about 45 cm above 1200-m elevation. Ash mantles deeper than 36 cm, and that meet several other NRCS criteria, are considered members of the order Andisols (Soil Survey Staff, 1999) or Andosols of the World Reference Base (FAO/ISRIC/ISSS, 1998).

Mean AT showed no significant decrease with increasing slope gradient (Figure 1.3). Mean AT showed little variation with a small range of 25 to 34 cm across all slope classes. Slopes <10 percent showed significantly less volcanic ash than all classes except the 60 percent class. Ash depth increases up to the 20-to-30 percent SLP class; after which, there are no significant differences in AT by SLP class. The 20-to-30 percent class had significantly greater ash depths than all slope classes and was marginally greater than the 40 to 50 percent class (p = 0.12).

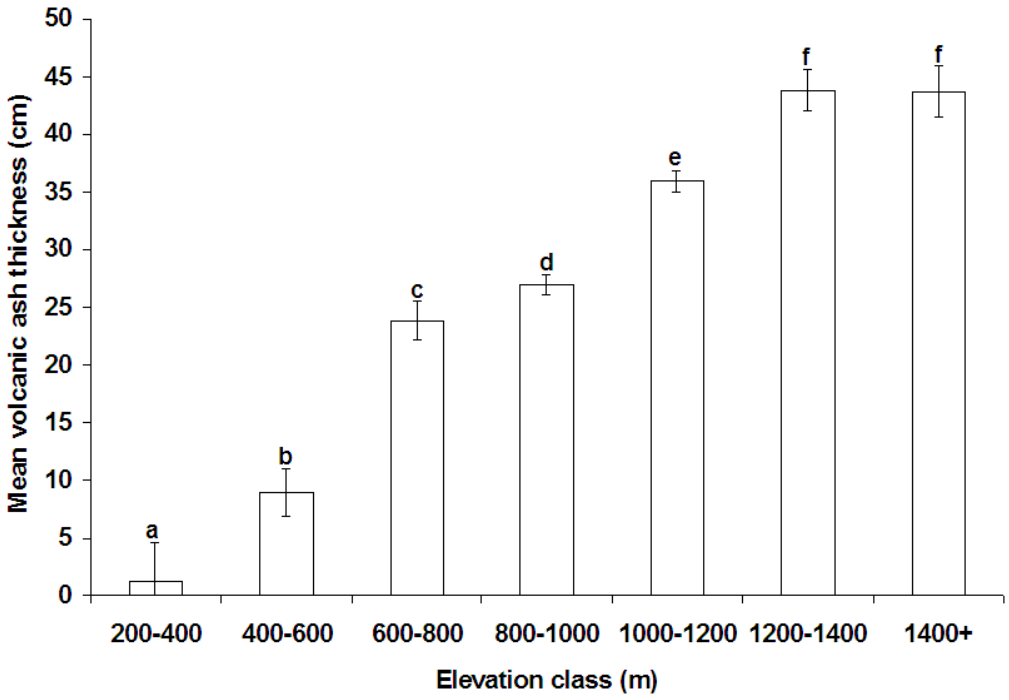

F**igure 1.2.** Mean volcanic ash thickness as a function of elevation class in north central Idaho. Y-axis bars represent standard errors, with letters indicating significant differences ($p < 0.1$).

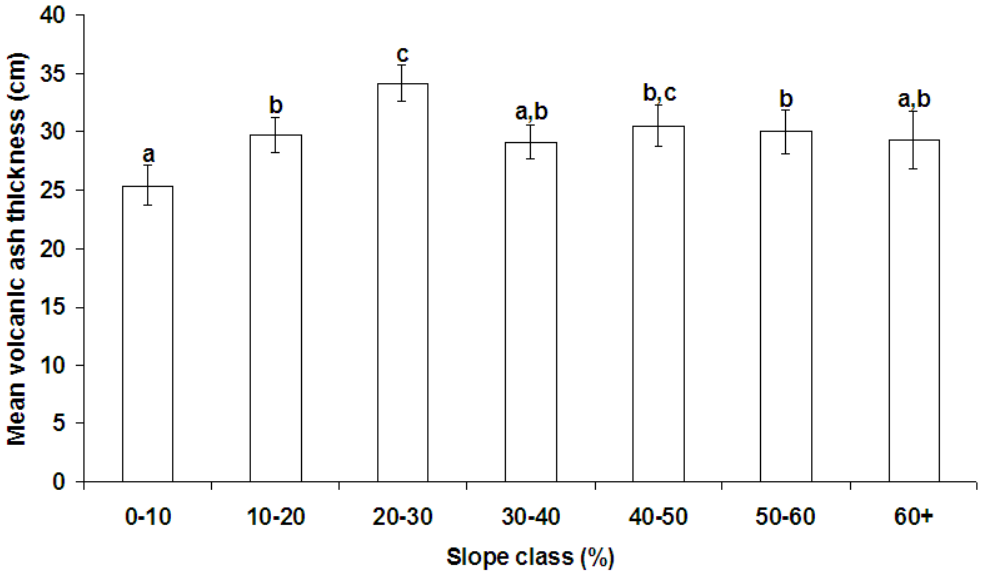

Figure 1.3. Mean volcanic ash thickness as a function of slope class in north central Idaho. Y-axis bars represent standard errors, with letters indicating significant differences ($p < 0.1$).

North aspects generally exhibit thicker ash mantles than south facing aspects (Figure 1.4). N, NW, and SE aspects show mean ash depths >32 cm. NE and W facing aspects have thinner ash caps (~30 cm), but are not significantly different than N, NW, or SE aspects. S, SW, and E aspects have significantly thinner ash mantles of about 27 cm.

Slope curvature shows that nonlinear surfaces retain a greater thickness of volcanic ash compared to linear surfaces (Figure 1.5). Concave and convex surfaces show mean ash depths >30 cm for both profile (PRCU) and plan (PLCU) surface curvature. Linear surfaces in both PRCU and PLCU are significantly lower (<25 cm) than either convex or concave surfaces. There was no statistical difference between concave and convex in either PRCU or PLCU slope curvature.

Vegetation series and habitat type plant associations showed the strongest relationship with AT (Figure 1.6). Overall, the ponderosa pine (PIPO) and Douglas-fir (PSME) vegetation series have very thin volcanic ash mantles (<3 cm) and show no significant change by habitat type within series. Grand fir (*Abies grandis* – ABGR [Dougl.] Lindl.) has the widest range in ash-influence of all vegetation series. Mean AT ranges from 0 to 40 cm depending on the underlying habitat type within series. The moist twinflower (*Linnaea borealis* – LIBO L.) habitat type of the ABGR vegetation series surprisingly shows no significant ash mantle (mean = 0 cm). AT in ABGR habitat types can be described as a function of increasingly moist understory indicator species, with the exception of LIBO. Habitat type rankings for AT would be *LIBO* < *PHMA/SYAL* < *CLUN* < *ASCA*; where PHMA, SYAL, CLUN, and ASCA represent ninebark (*Physocarpus malvaceus* [Greene] Kuntze), snowberry (*Symphoricarpus albus* [L.] Blake), queen-cup beadlily (*Clintonia uniflora* [Schult.] Kunth.), and wild ginger (*Asarum caudatum* Lindl.), respectively. These

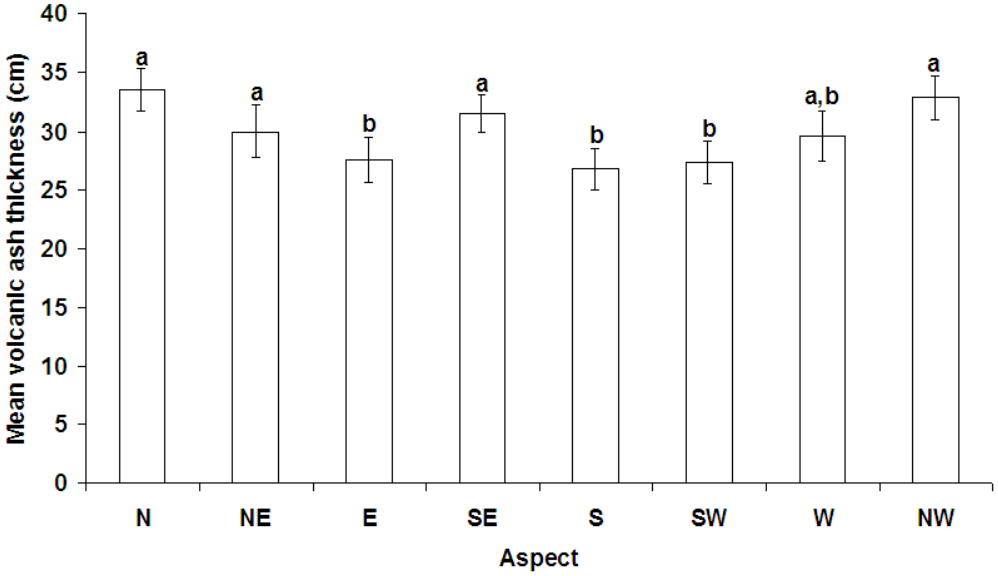

Figure 1.4. Mean volcanic ash thickness as a function of aspect class in north central Idaho. Y-axis bars represent standard errors, with letters indicating significant differences ($p < 0.1$).

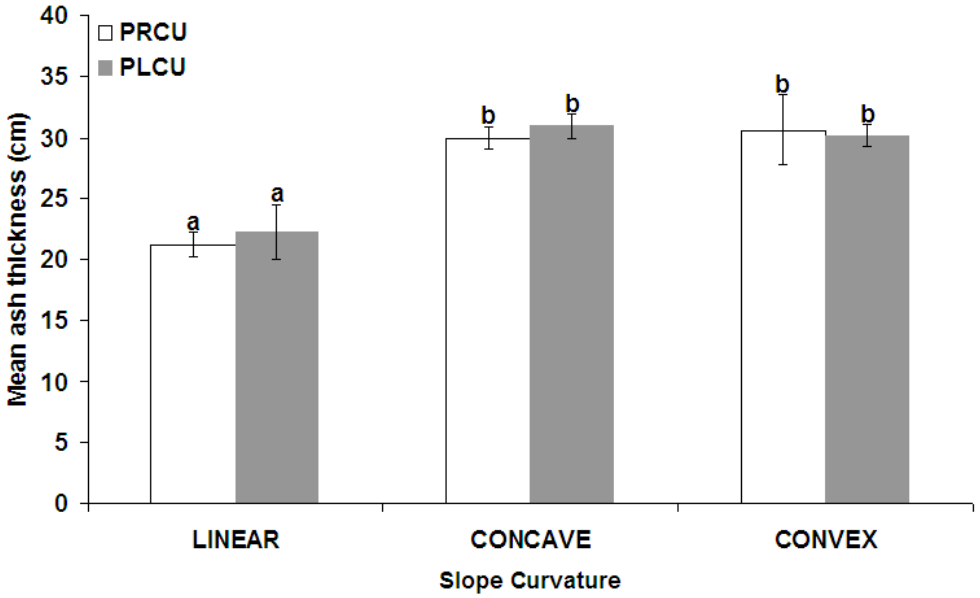

Figure 1.5. Mean volcanic ash thickness as a function of profile curvature class in north central Idaho.Y-axis bars represent standard errors, with letters indicating significant differences ($p < 0.1$).

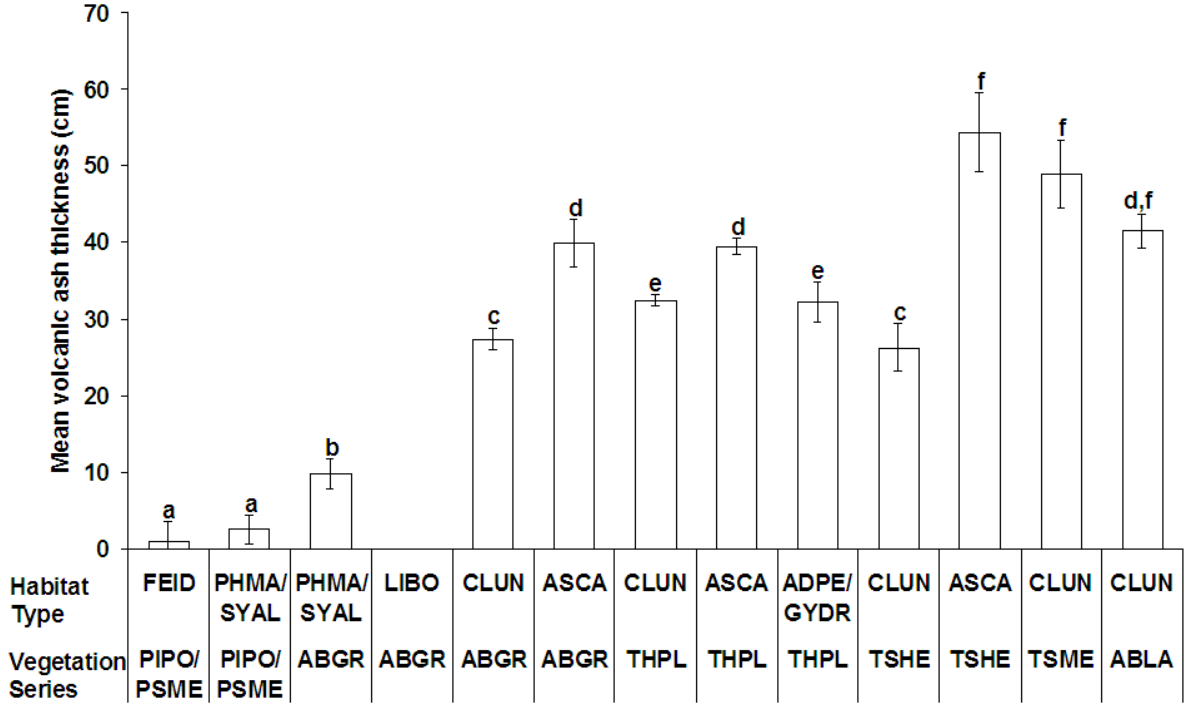

Figure 1.6. Mean volcanic ash thickness as a function of overstory and understory indicator plant species in north central Idaho. Y-axis bars represent standard errors, with letters indicating significant differences ($p < 0.1$) (Cooper et al., 1991).

rankings suggest that vitrandic intergrades would be more prevalent on PHMA/SYAL and LIBO habitat types, andic intergrades on CLUN, and Andisols on ASCA.

Changing from an ABGR to a western redcedar (THPL) vegetation series is accompanied by a 5-cm increase in mean AT when comparing across CLUN habitat types. This shift is not evident for the ASCA habitat type, which shows no significant differences between ABGR and THPL vegetation series. Maidenhair fern (*Adiantum pedatum* – ADPE L.) and oak-fern (*Gymnocarpium dryopteris* – GYDR [L.] Newm.) habitat types show a reduction of >7 cm in mean AT over ABGR/THPL-ASCA. Mean AT for CLUN and ADPE/GYDR habitat types suggest that andic intergrades would be most common, with Andisols (i.e., ash mantle >36 cm) occurring primarily under an ASCA habitat type. Based on these observations, understory rankings of habitat type by increasing AT would be *CLUN = ADPE*/*GYDR* < *ASCA*.

The western hemlock (TSHE) series displayed the largest difference in AT between CLUN and ASCA habitat types (~28 cm). TSHE-CLUN habitat types show at least a 6-cm decrease in mean AT when compared to THPL-CLUN, however a TSHE-CLUN habitat type would still fall within the andic intergrade classification associated with other CLUN habitat types. AT in the ASCA habitat type is significantly greater for TSHE vegetation series than for any other series with observed ASCA habitat types. Mean ash depths on TSHE-ASCA are 54 cm, which would place them well within the Andisol soil order.

Mountain hemlock (TSME) and Subalpine fir (ABLA) series are typically found at higher elevations where air temperatures are relatively low and annual precipitation high. The warmer, moister ASCA habitat was not observed. Mean AT is greater on TSME-CLUN than

ABLA-CLUN, but the difference is statistically insignificant. Volcanic ash-thickness on these vegetation series is >36 cm, thus placing them into the Andisol order.

Volcanic Ash Distribution Modeling

The class variables listed in Table 1.1 were added stepwise into a multiple linear regression equation. Variables were assumed to be independent and normally distributed. The final model, with selected variables acting as fixed effects on AT, is:

$$AT_{jklmno} = \mu + PRCU_j + ASP_k + SLP_l + ELE_m + VS*HT_n + \varepsilon_{jklmno} \quad \text{[Eq. 1.2]}$$

where,

AT_{jklmno} is the estimated ash thickness for observation *o* with vegetation series*habitat type interaction *n* at elevation *m* on slope *l* with aspect *k* and profile curvature *j*,

μ is overall volcanic ash thickness mean,

$PRCU_j$ is the fixed effect of profile curvature,

ASP_k is the fixed effect of aspect,

SLP_l is the fixed effect of percent slope,

ELE_m is the fixed effect of elevation in meters,

$VS*HT_n$ is the fixed effect of vegetation series*habitat interaction,

ε_{jklmno} is the error term;

where, $j = 3$ for profile curvature, $k = 9$ for aspect, $l = 7$ for slope, $m = 7$ for elevation, $n = 13$ for vegetation series*habitat type interaction, and $o = 1$ for number of observations per location.

All class variables listed in Table 1.1 explained a significant portion of variation in AT, except PLCU ($p < 0.1$) (Table 1. 2). Variables ranked from least to most in variance

Table 1.2. General linear regression model variables retained in a volcanic ash prediction analysis for a forested north central Idaho landscape. Partial variance indicates the percent of the model R^2 explained by each retained variable.

	Elevation	Slope	Aspect	Profile Curvature	Vegetation Series* Habitat Type
Partial Variance (%)	**18.2**	**4.7**	**4.2**	**1.7**	**71.2**
Significance†	**<0.0001**	**0.006**	**0.04**	**0.03**	**<0.0001**

† Significance level tested at α = 0.1.

explained are *PRCU* < *ASP* < *SLP* < *ELE* < *VS*HT*. The interaction term, VS*HT, accounted for the largest percentage of explained variance at 71.2 percent. ELE was the second largest at 18.2 percent. SLP and ASP accounted for 8.9 percent combined, and PRCU explained the least at 1.7 percent. The overall model was significant (p <0.001) and accounted for 60 percent of the observed variation in AT. A model RMSE of 10.7 cm and CV of 36 percent indicate that there is a significant amount of variation still unaccounted for; however, the model error is significantly lower than the variation found in local soil series.

DISCUSSION

Topographic and Vegetative Indicators

It is evident from the broad relationships presented that volcanic ash distribution is strongly associated with vegetation patterns and less dependent on terrain attributes. Elevation, although a terrain attribute, shows strong collinearity with local precipitation gradients and vegetative cover (data not shown). This situation suggests that elevation serves as a proxy variable for interactions between precipitation and vegetation patterns and their subsequent effect on ash distribution.

The historic role elevation played in volcanic ash deposition was probably two-fold. First, increasing elevation shifts vegetation series towards moister plant associations, thereby increasing vegetation cover and reducing erosional forces on initial ash deposits. Second, lush vegetation cover at higher elevations would retain wind-transported volcanic ash from drier regions to the west of the study area. Variability in ash thickness at these elevations may be attributable to redistribution occurring between initial deposition and understory establishment. This period of minimal understory ground cover may have facilitated colluvial and alluvial volcanic ash redistribution. It follows that at lower, drier elevations

unincorporated volcanic ash would have been more susceptible to both wind and precipitation erosion.

Slope class did not have a negative impact on mean AT with slopes >60 percent showing no significant decline in ash depths (Figure 1.3). The uniform distribution of mean AT across slope classes >30 percent indicates that increasing slope percent does not correspond with decreasing AT. This result supports other research on slope stability of volcanic ash. In a review of volcanic ash soils, Warkentin and Maeda (1980) note that volcanic ash on free-standing slopes are common in regions of high rainfall. They attribute this high degree of stability to the unique permeability of volcanic ash. However, site disturbance, low soil moisture, or discontinuities with buried subsoil surfaces are all factors that will enhance ash erosion on steep slopes (Warkentin and Maeda, 1980).

The significantly lower mean AT in the 0-to-10 percent slope class may be due to the geographic location of these observations. A majority of these observations for nearly flat terrain were on the benchlands of the south and southwest portion of the study area. This region is characterized by low elevation PSME and ABGR vegetation series, which often exhibit thin or mixed volcanic ash mantles. All remaining slope classes are uniformly scattered across the study area.

The prevalence of thicker ash mantles on north aspects may be attributable to several factors (Figure 1.4). North aspects typically support moister plant communities in our study area (Cooper et al., 1991). These moist plant communities may provide greater soil surface cover, which would decrease the impact of precipitation and overland water flow on volcanic ash redistribution. Additionally, the moisture retained within the soils after precipitation events would be less susceptible to evaporation from solar radiation. Oppositely, increased

solar radiation on southerly aspects may have contributed to soil moisture loss and ash erosion. Giest and Strickler (1978) found volcanic ash soils of Oregon to be susceptible to wind erosion once in a dry state. Assuming that current southwesterly prevailing wind patterns were similar to historic post-eruption patterns, dry volcanic ash on south-facing slopes would be expected to be more susceptible to redistribution by wind and overland water flow than north aspects. The significant increase in AT on southeast slopes is anomalous to this theory and suggests that the overall effect of aspect on ash distribution is local and intricately tied with surrounding topographic and environmental factors.

The significant decrease in AT on linear surfaces shown in Figure 1.5 is partially correlated with the slope class these observations share. A review of the dataset shows that about 67 percent of the linear surfaces occur on slopes <10 percent with the remainder unevenly divided among several steeper slope classes. As detailed in the previous discussion of slope classes, observations with gradients <10 percent are found primarily in the drier benchland portions of the study area. The correlation between slope steepness and slope surface curvature within the dataset may mask local effects of slope curvature on AT. Surprisingly, convex surfaces in both profile and plan positions displayed no significant decrease in mean AT over concave surfaces. Other research on volcanic ash deposition after the eruption of Mt. St. Helens has shown that concave surfaces support thicker ash mantles than convex (Zobel and Antos, 1991). Our conflicting results may be due to the level of variation found within these classes. Standard errors were small because of large sample sizes, but the standard deviations were often large within the surface classes, reflecting significant variation within the data.

Cooper et al. (1991) associate shifts in climax plant associations to distinctive soil and/or topographic microclimate features. Habitat type shifts and differing soil ash depth are evident across the broad habitat type associations observed in our study area (Figure 1.6). These strong relationships may be attributed to many combinations of topographic, climatic, or edaphic factors. However, two possible explanations are: 1) location of vegetation series within a precipitation-elevation continuum, and/or 2) topographic influence on volcanic ash redistribution. Zones on the moist end of the series spectrum should have thicker vegetative cover. Greater density of vegetative cover would entrap windborne ash and inhibit erosional redistribution. Scenario two suggests that erosional forces, influenced by topographic features, favored the accumulation of volcanic ash in certain landforms. Under these varying influences, it is probable that following the post-Mazama, mid-Holocene drought, volcanic ash enabled moister plant associations to inhabit landscape positions previously dominated by drier plant associations. Steele et al. (1981) noted that the influence of volcanic ash contributed to distinct shifts in Idaho plant communities. However, it is still an open question as to whether the presence of volcanic ash is responsible for shifts in plant associations, or that variations in plant community were responsible for differential ash retention. Despite this uncertainty, AT is highly correlated with plant associations.

PSME and PIPO vegetation series show the least AT within our data. Shifts to moister habitat types within these vegetation series show no significant dependence on volcanic ash. It has been suggested by regional soil scientists that these vegetation series now reside on landscapes that, post-Mazama eruption, were drier and did not support forest vegetation cover (Barker, 1981). Lack of overstory cover and dry climatic conditions prevented these landscapes from retaining volcanic ash mantles subsequent to the eruption.

AT in ABGR communities is highly variable. Unlike successively moister plant associations, an ABGR vegetation series does not always indicate the presence of significant volcanic ash-influence. This variability is partly attributable to the transition zone that ABGR inhabits between xeric and udic SMRs. ABGR plant associations in a xeric SMR would be associated with minimal to no ash-influence; whereas, an udic SMR would be associated with thicker ash mantles. This suggests that an increase in plant available soil moisture would shift the understory plant community towards moister habitat types. Thus, drier habitat types (PHMA/SYAL) often exhibit less ash influence in the soil than the CLUN and ASCA types.

An exception to this pattern is the ABGR-LIBO association. LIBO is considered to inhabit moister environments than PHMA, suggesting that volcanic ash might be present on this habitat type. The absence of volcanic ash on LIBO habitat types may be attributable to the fact that only five observations were collected within this habitat type, providing a poor representation of the range in AT. A second explanation may be that LIBO acts as a colonizer following site disturbance. Past management or biological activity may have displaced the volcanic ash from these locations creating a disturbed environment favorable to the establishment of a LIBO habitat type.

All remaining plant associations moister than ABGR show significant ash-influence in the soil. The presence of a thick ash mantle is often identified by the presence of these climax species. Increasing AT in the soil is evident in the habitat type gradients within the THPL series, however habitat type differences are minimal compared to those observed in ABGR and TSHE vegetation series.

The TSHE vegetation series occupies a narrow ecological range in north Idaho forests and primarily inhabits moist, moderate temperature sites. TSHE, as a species in this region, are

intolerant to drought, excess moisture, and frost (Cooper et al., 1991). The narrow ecological range suggests that other edaphic and climatic factors might play a larger role in TSHE distribution than volcanic ash-influence in the soil. Such factors may also explain why TSHE-CLUN plant associations have thinner ash mantles than THPL-CLUN. TSHE-ASCA plant associations do show a significant increase in AT. This result suggests that volcanic ash is associated with a shift to moister understory plant communities within the TSHE vegetation series.

TSME and ABLA plant communities occupy high elevation sites with up to 1500 mm of annual precipitation within our study area. Vegetation series within these zones are probably not dependent on the presence of volcanic ash for their establishment. The high precipitation and dense vegetative cover of these plant communities retained volcanic ash subsequent to original ash deposition.

Volcanic Ash Distribution Modeling

The strength of the relationships between elevation, plant communities, and volcanic ash produces a strong predictive ability for our ash distribution model. An R^2 value of 0.6 is considered an excellent improvement over the limited regional volcanic ash modeling attempts. Predictions from this model allow quantitative ash assessments with a known error within the study area. Natural resource managers can use this model to integrate the predictions into a GIS. One motivation behind developing a quantitative ash distribution model was to overcome the variation inherent within mapping units generated through a soil survey. Volcanic ash thicknesses in Hugus and Bouldercreek soil series commonly found in our study area, have mapped variations >20 cm (Soil Survey Division, 2006). The model's

RMSE of 10.7 cm significantly improves on this level of variation, thus providing a finer resolution support tool for local forest soil management.

Further research should be conducted to determine local affects of topographic features on ash distribution despite the significant improvement this model provides in predicting ash depth and distribution. Global statistical procedures such as MLR may mask local topographic influence. Adjusting a statistical model to perform a more local analysis may yield improved results. A more costly, but perhaps informative method, would be a detailed survey of a finite landscape. Research at local levels may reveal topographic and volcanic ash relationships otherwise masked by large conventional soil surveys. Regardless of which approach is used, modeling ash distribution seems to be inherently a local exercise. The extrapolation of model results outside our study area is not recommended. The concepts behind the model presented in this paper may be applicable elsewhere, but the relationships as reflected in the model parameter estimates are unique.

SUMMARY

This study's findings suggest that volcanic ash distribution is intricately linked with elevation and plant community associations. Elevation increases precipitation, which in turn supports different climax plant communities. Increasing plant density at each successive climax community may have served to retain ash deposits subsequent to volcanic eruptions and entrap wind-transported volcanic ash from drier, lower elevation sites. Topographic variables show little impact on ash thickness patterns. Several of the terrain attributes showed clustering by geographic location within our study area. Gentler slopes, which were predominately found at drier, lower elevations, supported thinner ash mantles. The slope curvature variable was also linked to geographic location. Observations with nonlinear slopes

were most often found in the mountainous region of the study area. The strong effect of elevation and plant associations reduced the ability to distinguish mean ash thickness differences between convex and concave surfaces.

Statistical modeling accounted for 60 percent of the observed variation in ash thickness and produced an RMSE of 10.7 cm. These model statistics indicate a significant development in the capability of estimating volcanic ash thickness. Model error was significantly lower than the variation of >20 cm often observed in local ash-influenced soil series. However, it became evident during our analyses that ash distribution and thickness is heavily influenced by local ecological and topographic attributes that cannot be assumed to affect ash depth uniformly across a study area. Future ash modeling efforts must focus on assessing local environmental influences and account for nonstationarity in the independent variables. Such an analysis may clarify the ecological and topographic effects on ash distribution and thickness that are otherwise generalized in a global regression analysis.

LITERATURE CITED

Bacon, C.R. 1983. Eruptive history of Mount Mazama and Crater Lake caldera, Cascade Range, USA. J. Volcanol. Geotherm. Res. 18:57-115.

Barker, R.J. 1981. Soil survey of Latah County area, Idaho. USDA – Soil Conservation Service. U.S. Govt. Print. Office. Washington, D.C.

Busacca, A.J., H.M. Marks, and R. Rossi. 2001. Volcanic glass in soils of the Columbia Plateau, Pacific Northwest, USA. Soil Sci. Soc. Am. J. 65:161-168.

Cooper. S.V., K.E. Neiman, and D.W. Roberts. 1991. Forest habitat types of northern Idaho: A second approximation. USDA For. Serv. Gen. Tech. Rep. INT-236. 143 p.

Dubroeucq, D., D. Geissert, and P. Quantin. 1998. Weathering and soil forming processes under semi-arid conditions in two Mexican volcanic ash soils. Geoderma 86:99-122.

FAO/ISRIC/ISSS. 1998. World Reference Base for Soil Resources. Food and Agricultural Organization of the United Nations, International Soil Reference and Information Centre, and International Society of Soil Science. World Soil Resources Report #84. Rome.

Geist, J.M., and G.S. Strickler. 1978. Physical and chemical properties of some Blue Mountain soils in northeast Oregon. USDA For. Serv. Res. Pap. PNW-236. 19 p.

Hironaka, M., M.A. Fosberg, and K.E. Neiman. 1991. The relationship between soils and vegetation. *In* A.E. Harvey et al. (ed.). Proceedings – Management and productivity of western montane forest soils. USDA For. Serv. Gen. Tech. Rep. INT-280. 254 p.

Hunter, C.R. 1988. Pedogenesis in Mazama tephra along a bioclimatic gradient in the Blue Mountains of southeastern Washington. Ph.D. Dissertation. Washington State Univ. Pullman. 128 p.

Idaho State Climate Services. 2000. Digital precipitation for Idaho: Average, monthly, and annual (1961-1990). Idaho State Climate Services. Moscow, ID.

McDaniel, P.A., M.A. Wilson, R. Burt, D. Lammers, T.D. Thorson, C.L. McGrath, and N. Peterson. 2005. Andic soils of the Inland Pacific Northwest, USA: Properties and ecological significance. Soil Science. 170:300-311.

Mullineaux, D.R. 1986. Summary of pre-1980 tephra-fall deposits erupted from Mount St. Helens, Washington State, USA. Bull. Volcanol. 48:16-26.

Nanzyo, M., S. Shoji, and R. Dahlgren. 1993. Physical characteristics of volcanic ash soils. *In* S. Shoji et al. (ed.). Volcanic ash soils: Genesis, properties, and utilization. Elsevier, Amsterdam. pp. 189-207.

Nimlos, T.J. 1980. Volcanic ash soils. Western Wildlands. 6:22-24

Nimlos, T.J., and H. Zuuring. 1982. The distribution and thickness of volcanic ash in Montana. Northwest Science. 56:190-197.

Shipley, S., and A.M. Sarna-Wojcicki. 1983. Distribution, thickness, and mass of late Pleistocene and Holocene tephra from major volcanoes in the northwestern United States: A preliminary assessment of hazards from volcanic ejecta to nuclear reactors in the Pacific Northwest. US Geol. Surv. Misc. Field Studies Map. MF-1435. Washington, DC. 27 p.

Soil Survey Division. March 2006. Official soil series descriptions. National Cooperative Survey. 19 March 2006. http://ortho.ftw.nrcs.usda.gov/cgi-bin/osd/osdname.cgi?-P.

Soil Survey Staff. 1999. Soil taxonomy. A basic system of soil classification for making and interpreting soil surveys. 2nd ed. USDA – Natural Resources Conservation Service. Agricultural Handbook No. 436. U.S. Govt. Print. Office. Washington, DC.

Steele, R., R.D. Pfister, R.A. Ryker, J.A. Kittams. 1981. Forest habitat types of central Idaho. USDA For. Serv. Gen. Tech. Rep. INT-114. 137 p.

Warkentin, B.P., and T. Maeda. 1980. Physical and mechanical characteristics of Andisols. *In* B.K.G. Theng (ed.) Soils with variable charge. Offset Publications. Palmerston North, NZ. pp. 281-301.

Williams, H., and G. Goles. 1968. Volume of the Mazama ash-fall and the origin of Crater Lake caldera: Andesite Conference Guidebook. Oregon Department of Geology and Mineral Industries Bulletin 62. pp. 37-41.

Wilson, J.P., and J.C. Gallant. 2000. Digital terrain analysis. *In* J.P. Wilson and J.C. Gallant (ed.). Terrain Analysis: Principles and Applications. John Wiley and Sons, New York. pp. 1-27.

Zdanowicz, C.M., G.A. Zielinksi, and M.S. Germani. 1999. Mount Mazama eruption: Calendircal age verified and atmospheric impact assessed. Geology 27:621-624.

Zobel, D.B., and J.A. Antos. 1991. 1980 tephra from Mt. St. Helens: Spatial and temporal variation beneath forest canopies. Biol. Fertil. Soils. 12:60-66.

CHAPTER 2: Volcanic Ash Distribution and Thickness in a Forested North Central Idaho Landscape

ABSTRACT

Many forest soils of north central Idaho contain thick mantles of volcanic ash. However, there is little information that quantitatively defines the influence of terrain attributes on volcanic ash distribution and thickness. We assessed the influence of terrain attributes on volcanic ash distribution with multiple linear regression (MLR) and geographically weighted regression (GWR). MLR showed that elevation (ELE) and slope (SLP) were significantly related to soil ash thickness (AT) ($p = 0.05$). Compound terrain attributes associated with erosion and deposition landscape positions were insignificantly correlated with AT ($p > 0.1$). Although ELE and SLP were statistically significant, they accounted for only 28 percent of the overall variation in AT. A GWR analysis found that ELE, SLP, plan curvature (PLCU) and wetness index (WIN) were significantly related to volcanic ash distribution ($p = 0.05$). GWR showed that ELE, PLCU, and WIN were nonstationary, which indicates that a specific independent variable value influences AT differently depending on geographic location. Results suggest that the effects of PLCU and WIN on AT are dependent upon elevation and mean annual precipitation. GWR model fit and precision improved by 36 and 30 percent, respectively, over the MLR model. An ash distribution and thickness map was created, using the GWR results, to provide information for natural resource managers.

INTRODUCTION

Forest soils of the Inland Northwest, USA are commonly influenced by eolian deposition. Over the last several millennia volcanic eruptions from the Cascade Mountain Range periodically blanketed this region with volcanic ash depositions (Mullineaux, 1986; Richmond et al., 1965; Ruhe and Olson, 1980; Shipley and Sarna-Wojcicki, 1983). The most recent significant eruptive event was that of Mt. Mazama (now Crater Lake, OR) approximately 7600 yr BP (Zdanowicz et al., 1999). Estimates suggest that >116 km^3 of volcanic tephra was ejected during this one event (Bacon, 1983). Regional forest soils display a range of ash influence from mixed to a relatively pure ash mantle (Busacca et al., 2001; Brown and Loewenstein, 1978; Geist and Strickler, 1978). Soils that exhibit mixing or relatively shallow ash mantles (i.e., <36 cm) are often characterized as andic or vitrandic intergrades of other orders (Gardner, 2005; McDaniel et al., 2005). Ash mantles >36 cm and relatively pure, are often classified as Andisols in Soil Taxonomy (Soil Survey Staff, 1999) and Andosols in the World Reference Base (FAO/ISRIC/ISSS, 1998).

A recent study of volcanic ash distribution and depth across the Columbia Plateau of eastern Washington State found that Mt. Mazama ash had a fairly uniform thickness of approximately 15-20 cm upon initial deposition, with thinning in areas more distal to the eruption (Busacca et al., 2001). This suggests that a thinning, but fairly uniform ash mantle also occurred across the forested landscape of North Idaho. However, it is uncertain what role vegetation density played in volcanic ash retention at the time of the eruption. We can theorize vegetation effects were significant from a study completed by Zobel and Antos (1991), in which they found that volcanic ash retention after the eruption of Mt. St. Helens was greater under forest canopies than in forest openings. Forest canopies tended to

temporarily trap volcanic ash, which over time was transported to the surface through precipitation or wind action. Further, forest canopies may have reduced the erosional losses of unincorporated volcanic ash due to overland water movement (Busacca et al., 2001).

The resistance of volcanic ash mantles to water erosion is relatively high because of its permeability (Warkentin and Maeda, 1980). Warkentin and Maeda (1980) argue that surface erosion due to slope gradient is not always the issue, but slope instability. Volcanic ash deposits, which are commonly found on steep forested slopes, are often susceptible to mass movements such as landslides, slumps, or soil creep. Additionally, the drier layers of volcanic ash are more susceptible to these mass transport mechanisms due to low cohesion. Oppositely, Nammah et al. (1986) studied rill erosion rates of unincorporated volcanic ash following the 1980 eruption of Mt. St. Helens in southwest Washington, Their results showed that ash mantles dominated by silt-sized particles formed a slight crust that reduced surface erosion at shallow slopes, but as expected, erosion rates increased proportionally with slope gradient.

Low cohesiveness and disturbance enhance the susceptibility of volcanic ash to wind and water displacement (Warren, 1979). Consequently, silty volcanic ash is more likely to be displaced when disturbed during droughty periods (Buol et al., 2003; Cullen et al., 1991; Warkentin and Maeda, 1980). This suggests that volcanic ash deposited in the region immediately preceding a mid-Holocene drought (7600 – 5000 yr BP), would be susceptible to considerable reworking by wind following periods of wetting and drying of the surface ash layer (Hunter, 1988).

Soil formation was understood by Jenny (1941) to be a function of climate, parent material, topography, biotic influences, and time. Climatic variables exert controls at too

coarse of scale to be incorporated into this study; conversely, biotic influences exert a scale too fine to be practically defined. Consequently, in our study we focus on topography and the influence it exerts on the current distribution of volcanic ash parent material.

Extensive efforts have been undertaken within the past 20 years to spatially and quantitatively link soil attributes with topographic features to develop quantitative relationships that may then be used for spatial prediction (Gessler et al., 1995; Florinsky et al., 2002; McKenzie and Ryan, 1999; McSweeney et al., 1994; Moore et al., 1993a,b; Ryan et al., 2000). Topographic features have commonly been subdivided into primary and secondary attributes. Primary terrain attributes are often used to characterize catenary features such as hillslope form and position, and catchment area. Specifically, these attributes include elevation, slope, aspect, curvature, and profile contributing area. Secondary attributes are derived from two or more primary attributes. These attributes are used to describe the role of topography in redistributing water over and within a landscape. Consequently, secondary attributes can characterize the susceptibility of soil surfaces to erosion and deposition. The most common of these secondary attributes used in quantification are the wetness and stream power indices (Wilson and Gallant, 2000).

Digital terrain models (DTMs) have been widely used over the past several decades to model soil process and pattern associations across landscapes. DTMs model these associations by correlating digital representations of primary and secondary topographic attributes with soil features. Correlations between soil and landscape features are subsequently built into a statistical model that could be used to predict soil features at unknown locations (Florinsky et al., 2002).

Numerous studies have shown that these relationships are useful in predictive models. McBratney et al. (2003) provide an excellent review of these efforts. Moore et al. (1993b) found the wetness index to be highly correlated with horizon depth, silt percentage, organic matter content, and phosphorus. Gessler et al. (1995) showed plan curvature and the wetness index to be highly correlated with A horizon depth and solum depth. These results suggest that developing volcanic ash relationships with terrain attributes may be possible.

Multiple linear regression (MLR) is a common statistical method for predicting soil features across the landscape (McBratney et al., 2003). MLR assumes that each independent variable brought into a model affects the dependent variable uniformly (i.e., the assumption of stationarity) across the study area (Fotheringham et al., 2002). For example, MLR will assume that a slope curvature of "X" will have the same affect on "Y" (ash thickness, AT) at point "A" as at point "B". Hypothetically, MLR may not account for the fact that point "B" is located within a region that receives higher mean annual precipitation than point "A". Higher MAP may increase the potential for thicker ash mantles in concave landscape positions. Shifts in MAP may change the sign or slope of the slope curvature coefficient. This shift or sign change may not be shared by point "A", hypothetically found in a lower MAP region. Consequently, what is actually two separate curvature effects on AT is modelled within MLR as a single curvature effect. The result is a curvature coefficient with a large standard error and potentially imprecise estimates of AT. MLR is incapable of capturing the spatial complexity of landscape interactions at the local level.

A form of multiple linear regression that avoids this assumption while providing a measure of local variation in the independent variables is geographically weighted regression (GWR). GWR as developed by Fotheringham et al., (2002), relies on a form of kernel

regression within a MLR framework to develop local, as opposed to global, relationships between the dependent and independent variables. The development of local relationships facilitates an exploratory analysis of the stationarity assumption of a global MLR model. The subsequent derivation of spatial maps representing parameter estimate nonstationarity and spatial estimates of AT using the GWR method has to our knowledge never been attempted.

Therefore, the objectives of this study were to: i) assess the differences between GWR and MLR model AT estimates in a north central Idaho forest, ii) test nonstationarity in the independent variables, iii) determine if a GWR analysis enhances our understanding of terrain attribute influence on AT, and iv) derive a spatial display of GWR AT estimates.

MATERIALS AND METHODS

Study Area

The study area of ~ 205,000 ha is located within the ID-612 soil survey of north central Idaho, which stretches along the west slopes of the Clearwater Mountains and east of the Columbia Basin. Distal separation from Mt. Mazama ranges from ~ 600 to 670 km. Landscapes are generally classified as mountainous, with elevations ranging from 300 to 1800 m. Dry, low-elevation canyons and benchland dominate the southern portion of the area, with MAP approaching 300 mm (Idaho State Climate Services, 2000). Progressing northward, topography rapidly changes to high mountain ridges and valleys (MAP ~ 1500 mm). Soil parent material varies widely from metasedimentary schists and quartzites to igneous granites and basalts. Eolian deposits of loess from the Columbia Basin and volcanic ash from the eruption of Mt. Mazama are often found as intermixed mantles. Vegetation patterns reflect the dramatic shift in topography and climatic regimes. Ponderosa pine (*Pinus ponderosa* Dougl.) habitat types are found predominately in the southern portion of the study

area, while western redcedar (*Thuja plicata* Donn) and western hemlock (*Tsuga heterophylla* [Raf.] Sarg.) can be found to the north (Cooper et al., 1991).

Data Collection

Six hundred and seventy-one soil-site descriptions and their spatial coordinates from within the ID-612 soil survey were obtained from the Orofino, ID NRCS field office (Figure 2.1). Soil-site description locations were selected by NRCS field soil scientists to support the ID-612 soil survey. Records were collected by ~ five lead soil scientists over ~ 15 years. Location coordinates for the majority of the data were transcribed from aerial photos to a GIS. A small portion of the records was established using a geographic positioning system (GPS) device toward the end of the soil survey. For those locations obtained from aerial photos, we assumed the accuracy to be within the cell size of a United States Geological Survey (USGS) 30-m digital elevation model (DEM).

Soil-site description locations were established to capture the range in terrain and soil property characteristics established for a soil series. Each soil series was created based on landscape features that showed similar soil development. Soil measurements were collected from 1-m soil pits established at each soil series characterization location. Soil horizons were described and recorded. Site descriptors were collected by: 1) clinometer (slope), 2) compass (aspect), 3) visual classification (slope curvature), and 4) topographic map (elevation). Often, terrain attributes in this data set were inconsistently observed, which reduced the number of observations available for analysis. Therefore, primary and secondary terrain attributes were computed from a USGS 30-m DEM (Table 2.1). Plan and profile slope curvature (PLCU, PRCU), wetness index (WIN), stream power index (SPI), stream transport index (STI), and

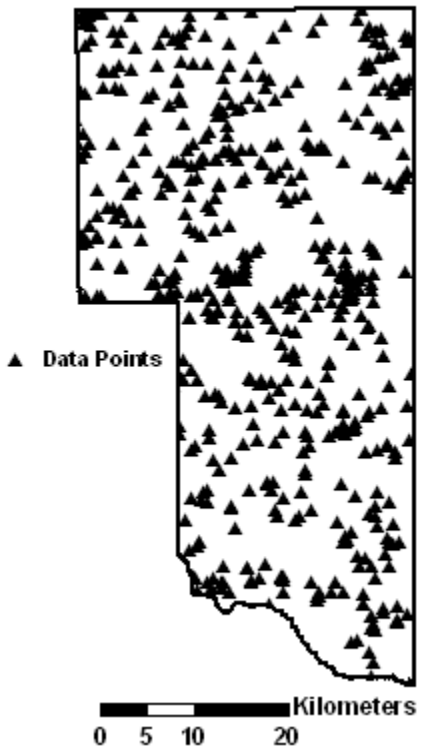

Figure 2.1. Distribution of 671 NRCS soil-site observations in a north central Idaho landscape.

Table 2.1. Summary of collected site and terrain attributes for 671 observations in a forested north central Idaho landscape (†Wilson and Gallant, 2000).

Site Variables	Code	Min.	Mean	Max.	Significance
Soil Morphological					
Ash Thickness (cm)	**AT**	**0**	**10.3**	**29**	**Drought stress buffer for plant community**
Terrain Attributes†					
Elevation (m)	**ELE**	**295**	**957**	**1677**	**Climate, vegetation cover**
Slope (%)	**SLP**	**0**	**29**	**82**	**Surface water velocity**
Aspect (°)	**ASP**				**Solar irradiation, wind erosion/deposition**
Compound Terrain Attributes†					
Profile Curvature	**PRCU**	**-6.47**	**0.02**	**7.69**	**Erosion/deposition rate**
Plan Curvature	**PLCU**	**-8.35**	**0.02**	**4.37**	**Converging/diverging flow**
Wetness Index	**WIN**	**0**	**9.10**	**23.02**	**Contributing upslope area**
Stream Power Index	**SPI**	**-180057**	**1440**	**441909**	**Net erosion/deposition**
Sediment Transport Index	**STI**	**-12633**	**158**	**21289**	**Slope length influence**
Solar Insolation	**SOLAR**	**739**	**4279**	**5839**	**Slope/aspect interaction**

solar insolation (SOLAR) were derived from a DEM larger than the study area to account for terrain influences beyond the study area boundaries. Grid based computations of terrain attributes were performed using the ArcGIS® INFO GRID command line. Grid values were extracted to the soil profile XY coordinates using a spatial analysis tool in ArcGIS ArcMAP ®. Field observed terrain attributes were subsequently used for validation of DEM-derived terrain attributes.

Statistical Analyses

Model variable measurements listed in Table 2.1 were assumed measured without error. This assumption was taken with caution, because of the reliance on: 1) soil data collected over a period of time by different field soil scientists, and 2) DEM-derived data with an accuracy of 30-m. Measurement error can lead to an inflated model error term, thus underestimating the *F*-statistic. This may lead to the elimination of variables that may have been significant if measured without error. Consequently, it cannot be assumed that insignificant independent variables have no effect on AT, because of potential observation and/or imputed error during data collection.

Two statistical analyses were performed to model the relationship between terrain attributes and AT. The first statistical model was developed using a stepwise MLR analysis. Significance of terrain attributes was based on estimated *t*-values for the parameter estimates and their associated standard errors. We used a significance level of 0.1 to retain independent variables in the model. A predictive equation was developed from the selected independent variables of the following general form:

$$AT_{(i)} = \beta_0 + \beta_1 X_{1(i)} + \beta_2 X_{2(i)} + \ldots + \beta_k X_{n(i)} + \varepsilon_i \quad \text{[Eq. 2.1]}$$

where $AT_{(i)}$ = predicted ash thickness at observed point *i*, β_k = k^{th} global parameter estimate; $X_{k(n)}$ = k^{th} independent variable value at the n^{th} location; and ε_i = model error at point *i*. Overall model fit and performance was assessed through the adjusted coefficient of determination (R^2_A) and root mean square error (RMSE).

The second statistical model was developed using GWR. Version 3.0 of GWR ® software was used (GWR, 2005). GWR is a relatively new statistical technique and has predominately been used in the social sciences. However, the general premise of GWR that parameter estimate stationarity is not always a valid assumption may also apply to landscape spatial analysis. Brundson et al. (1996) outline various cases where a global regression model does not adequately explain relationships between variables. They proceed to illustrate how structure within the independent variables often negates the value of such global models to explain or predict a dependent variable. Consequently, Fotheringham et al. (2002) developed GWR, which is loosely based on kernel regression, to explore nonstationarity within parameter estimates. GWR utilizes the multiple regression formulaic approach, but it allows parameter estimates to vary by geographic location. The general equation formula for GWR, as applied in this study, is stated as follows:

$$AT_{(i)} = \beta_{0(i)} + \beta_{1(i)} X_{1(i)} + \beta_{2(i)} X_{2(i)} + \ldots + \beta_{k(n)} X_{k(n)} + \varepsilon_i \quad \text{[Eq. 2.2]}$$

where $AT_{(i)}$ = predicted ash thickness at observed location *i*; $\beta_{k(n)}$ = k^{th} local parameter estimate at the n^{th} location; $X_{k(n)}$ = k^{th} independent variable value at the n^{th} location; and ε_i = model error at location *i*.

The loose similarity to kernel regression arises from the development of a search neighborhood approach (i.e., bandwidth) used to develop local parameter estimates.

Bandwidths can be considered as smoothing functions of the local parameter estimates. Caution must be exercised when deriving bandwidths. Large bandwidths can oversmooth the parameters, reducing the ability to capture local variability in the independent variables. Oppositely, small bandwidths produce parameter estimates with large local variation, reducing the ability to assess trends within the data (Fotheringham et al., 2002).

Bandwidths can be determined through several methods: 1) cross-validation (CV), 2) Akaike's Information Criteria (AIC), and 3) user-defined. The CV and AIC methods calculates the optimum bandwidth that minimizes either score. User-defined bandwidths allow analysts familiar with the data to change the bandwidth to build localized regression analyses. The bandwidth is then applied in an iterative manner across a study area. Observations that fall within this bandwidth are then used to create a localized regression analysis.

GWR provides for a fixed or adaptive approach to deriving bandwidths. Fixed bandwidths are developed using previous knowledge of spatial autocorrelation within the data and are implemented using the scalar units of the study area. Adaptive bandwidths similarly rely on user knowledge of the study area, but allow the bandwidth to vary across the study area. The adaptive technique relies on either an absolute or relative number of observations to be included within the localized regression. Consequently, the bandwidth will vary depending on the concentration of observations around the regression point. In geographic areas with a high concentration of data points, bandwidths will decrease. Oppositely, in areas with a low density of observations, bandwidths are allowed to expand to meet the defined percentage or number of observations.

Each observation within a selected bandwidth is then weighted by distance from the regression point and its influence on the local parameter estimate calculated. Points nearer the regression point are weighted heavier than those points located farther away (Fotheringham et al., 2002). This differs from weighted least-squares analysis (WLS), which attempts to address local variance by adjusting the parameter estimates by a matrix of error variances (Myers, 1990). We used a fixed, user-defined bandwidth based upon: 1) a fairly uniform distribution of data points, and 2) a predefined spatial autocorrelation analysis of our study area.

Regression models built using either bandwidth approach can then be compared against the global MLR model using various test statistics. The two primary statistical tests employed in GWR for model comparisons are the *F*-statistic and reduction of the AIC score. The *F*-statistic is the residual sum of squares for the global regression model divided by those of the GWR model. This "*F*-ratio" is then tested with the two models' respective degrees of freedom (*df*). The upper 0.1 percentile of the *F*-distribution was chosen as the significance level for our study.

The AIC score reduction test measures the information distance between model distribution *g* and the true distribution *f*. A comparison of this quantity between differing models $g_1, \ldots, g_n$, can be used to assess which model more closely represents the true distribution. Relative improvements of the AIC criteria >3 are associated with genuine differences between the global and local models. Score reductions <3 in the local model could be attributable to sampling error and are therefore not considered to be a significant improvement over the global model (Fotheringham et al., 2002). Minimization of AIC by >3, and a significant *F*-statistic suggest that there is structure to selected parameter estimates of

the independent variables. For our study, both the *F*-statistic and AIC score minimization were used to decide the significance of the "localized" regression model. Overall model fit and performance was assessed through the R^2_A statistic and RMSE.

GWR utilizes several statistical tests to determine if the variation in the parameter estimates is significant. For our study, a Monte Carlo significance test was used (Hope, 1968). The Monte Carlo test calculates the observed variance of local parameter estimates, which is then compared against 99 simulated sets of variances obtained through randomizations of the observed data. *p*-values are then computed for each variable parameter estimate.

Once a localized regression model was fitted that met the overall model and parameter significance requirements, parameter surfaces were interpolated using a deterministic inverse distance weighted function (IDW) to display the nonstationary effects of parameter estimates on the dependent variable – AT. A map of volcanic ash distribution and thickness was subsequently generated using a modified form of Equation 2.2 as follows:

$$AT^*_{(i)} = \beta^*_{0(i)} + \beta^*_{1(i)} X_{1(i)} + \beta^*_{2(i)} X_{2(i)} + \ldots + \beta^*_{k(i)} X_{k(i)} \quad \text{[Eq. 2.3]}$$

where $AT^*_{(i)}$ = predicted ash thickness at *unknown* location *i*, $\beta^*_{k(i)}$ = interpolated *k*th parameter estimate at location *i,* and $X_{k(i)}$ = *i*th observation of the *k*th independent variable.

RESULTS AND DISCUSSION

A correlation analysis showed no significant relationship between AT and the independent variables ASP, PRCU, PLCU, SPI, STI, and SOLAR and these were subsequently dropped from further correlation analysis. ELE, SLP, and WIN were significantly correlated with AT. A matrix of partial correlation coefficients of significant variables and their scatterplots are

shown in Figure 2.2. Smoothed curves were fitted to the scatterplots to indicate trends in the data. Correlation coefficients below the diagonal indicate that ELE is strongly correlated with AT (r = 0.5***). The smoothed curve for ELE indicates that AT increases linearly with increasing elevation. A comparison of a classed digital elevation and interpolated AT values distinctly shows thicker ash mantles at higher elevations (Figure 2.3a,b). This positive relationship between ELE and AT can potentially be associated with: 1) wind redistribution during dry climatic periods, 2) dense vegetation cover at higher elevations, and/or 3) soil redistribution following initial deposit on steeper, complex slopes. The silty texture of volcanic ash allows it to be easily re-entrained and transported downwind from drier regions to the west of our study area. Wind patterns typically flow in a northeasterly direction in this region, thus the higher reaches of the study area would trap the re-entrained volcanic ash. Additionally, the orographic effect increases vegetation cover at higher elevations, thus serving to protect volcanic ash deposits from further wind or water erosion. However, it should be noted that extensive reworking of the initial volcanic ash deposit at these higher elevations might have occurred during the period between initial deposition and understory establishment. Colluvial and/or alluvial forces from high precipitation and topographic relief may be partially responsible for these thicker ash mantles.

SLP shows a weak, but significant correlation with AT (r = 0.12**). The smoothed curve for SLP suggests that slope gradients <45 percent do not negatively affect the distribution of volcanic ash. However, the curve indicates that AT decreases on slopes >45 percent. The overall positive relationship supports findings by Warkentin and Maeda (1980) who noted stable ash mantles on slopes up to 70 degrees in high precipitation regions. These findings

suggest that soil surface erosion through wind or overland water flow is not a significant factor in volcanic ash redistribution on slopes <45 percent.

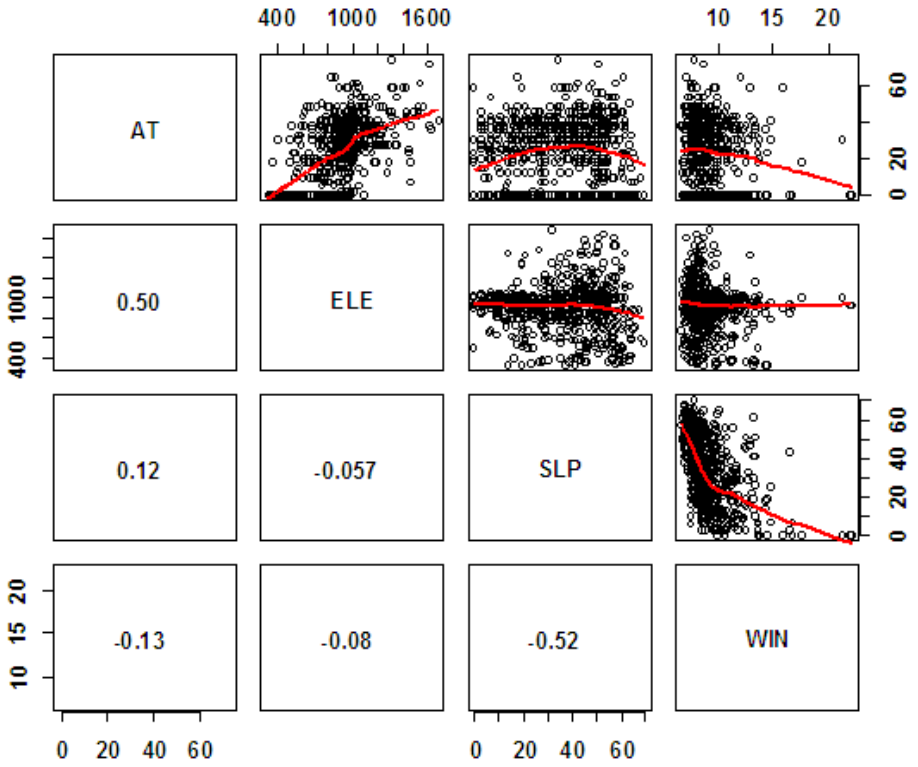

Figure 2.2. Partial correlation coefficient scatterplot matrix for selected primary and secondary terrain attributes versus volcanic ash thickness in a a forested north Idaho landscape.

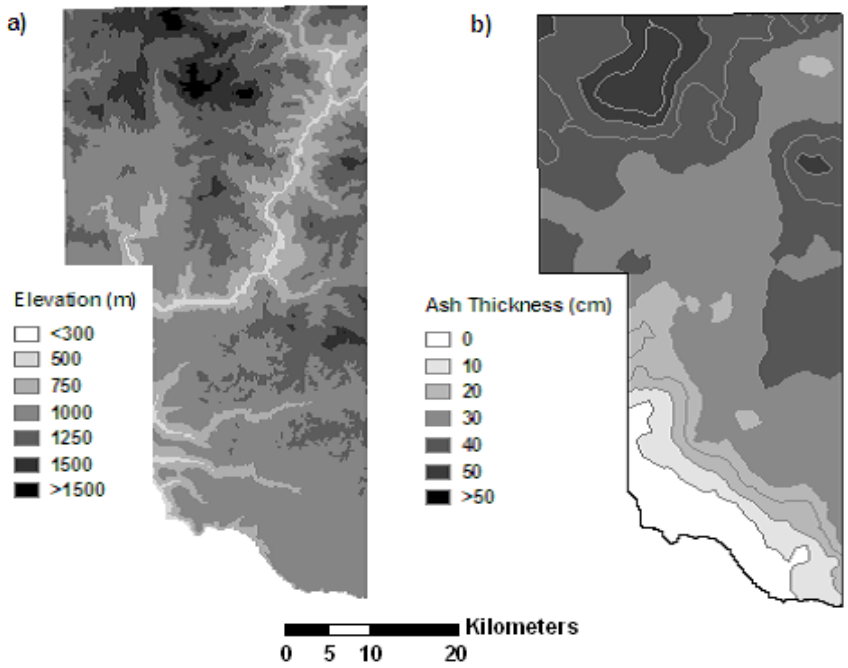

Figure 2.3. a) Elevation classes from a digital elevation model for the study area in north central Idaho, b) Interpolated ash thickness from 671 observations in a forested north central Idaho landscape.

WIN, which measures the upslope contributing area, shows a weak, but significant relationship with AT (r = -0.13**). WIN values <10 show relatively little influence on AT, but values >10 show a steady decline. This change in the relationship seems reasonable, because WIN values >10 are usually associated with dendritic drainage patterns within the study area. Consequently, surface mantles of volcanic ash would be exposed to greater erosive forces and potential redistribution or mixing in these areas.

Multiple Linear Regression Modelling

Given the pair-wise relationships described above, we developed an AT predictive model using MLR. Parameter estimates and model fit statistics were determined through a stepwise selection process and are provided in Tables 2.2 and 2.3. Only ELE and SLP were shown to significantly predict AT (p = 0.1), and these variables explained only 28 percent of the variation in AT. Consequently, the model RMSE value is 14.7 cm, which is 62 percent of the mean AT. An RMSE of this magnitude will provide poor predictive modelling. Volcanic ash classification typically divides ash thicknesses by 18-cm increments. Vitrandic suborders are classed at 0-18 cm, andic suborders at 18-36 cm, and Andisols at >36 cm. A 14.7 cm RMSE indicates that this model could erroneously classify volcanic ash soils.

Field observations suggested that AT was greater in aggradation areas across the landscape. Therefore, we expected that secondary terrain attributes would have been significant in the regression model. Preliminary exploratory data analysis showed that our data adequately represented the terrain attribute variation within our study area. Consequently, we felt that: 1) the overwhelming effect of ELE on AT may be masking underlying relationships between AT and other terrain attributes, and 2) potential spatial autocorrelation of AT values were leading to an underestimation of model variance.

Table 2.2. Predictive statistics of volcanic ash thickness from terrain attributes using multiple linear regression in a forested north central Idaho landscape.

MLR Coefficients	Estimate	*t*-value	*p*-value
Intercept	**-4.89**	**-2.49**	**0.05**
ELE	**0.005**	**15.49**	**<0.01**
SLP	**0.05**	**3.01**	**0.05**

Table 2.3. Volcanic ash thickness model fit statistics for multiple linear regression and geographically weighted regression in a forested north central Idaho landscape.

Regression Model	RMSE	R^2	Adjusted R^2	AIC
MLR	**14.7**	**0.28**	**0.28**	**4262**
GWR	**10.4**	**0.75**	**0.64**	**4141**
GWR Improvement	**4.3**	**0.47**	**0.36**	**121**

Underestimation of model variance inflates parameter *t*-tests (e.g., ELE and SLP at the expense of other terrain attributes) and reduces their confidence intervals. We undertook a localized regression analysis using GWR as developed by Fotheringham et al. (2002) to assess this possibility. This approach spatially decomposes the landscape in order to account for locational instability in model parameters.

Geographically Weighted Regression Modelling

A spatial autocorrelation analysis of observed AT values indicated that observations adjacent to each other shared similar AT values (*Moran's I* = 0.76) (Moran, 1950; Ord and Gettis, 1995). Subsequent modeling of this spatial autocorrelation indicated that a lag distance of approximately 2500 m captured the spatial structure in the dataset (data not shown). Therefore, we used this value as the user-defined, fixed bandwidth kernel for the localized GWR regression analysis.

A two-step process was used to determine significant variables. First, a stepwise selection process, similar to MLR, was implemented to determine which terrain attributes showed significant correlation with AT. If a variable was found to be globally insignificant ($p > 0.1$), a Monte Carlo analysis was then performed to determine if the insignificance could be attributed to nonstationarity of the parameter estimate. Attributes that showed global insignificance, but exhibited significant spatial nonstationarity, were retained for subsequent model development. Terrain attributes that met these criteria are shown with their associated ranges of parameter estimates and Monte Carlo nonstationarity *p*-values in Table 2.4.

GWR analysis showed ELE and SLP were globally significant ($p = 0.05$). PLCU, which is related to convergent and divergent water flow, was found to be mildly insignificant ($p = 0.15$). WIN, a measure of moisture accumulation as a function of upslope contributing area,

Table 2.4. Summary of geographically weighted regression parameter estimates and associated stationarity statistic for terrain attributes in a forested north central Idaho landscape.

Parameter	Min.	Lower Quartile	Median	Upper Quartile	Max.	Monte Carlo *p*-value
ELE	**-0.010**	**0.000**	**0.002**	**0.004**	**0.070**	**<0.01*****
SLP	**-0.265**	**-0.055**	**-0.007**	**0.045**	**0.297**	**0.49†**
PLCU	**-9.071**	**-1.035**	**-0.071**	**0.561**	**5.034**	**0.05***
WIN	**-4.355**	**-0.393**	**-0.019**	**0.501**	**4.705**	**0.05***

† Globally significant (*p* = 0.05).**

showed no global significance ($p = 0.25$). Although, PLCU and WIN were shown to be globally insignificant, a Monte Carlo simulation of parameter estimate variances found that these parameter estimates were significantly non-stationary ($p \leq 0.05$) (Table 2.4). ELE showed strong evidence of nonstationary ($p = 0.001$), while SLP was highly stationary ($p > 0.05$). Thus, the variance in the parameter estimates for ELE, PLCU, and WIN are attributable to structure within these variables and not due to randomness. Conversely, the local variation of SLP parameter estimates is due to randomness and not to any inherent spatial structure.

ASP, PRCU, SPI, STI, and SOLAR were shown to be insignificant at both the global and local level ($p > 0.1$). Overall, the GWR model explained 64 percent of the variation in AT. An *F*-test yielded a value of 4.3, which was significant at the 0.1 percent distribution level. Additionally, the local GWR model significantly reduced the global MLR AIC score by 121 points. Comparison of the model RMSE values shows that the GWR model reduced the RMSE over the MLR model by ~ 30 percent (Table 2.3).

We conclude that GWR significantly improves the explanation of variation in AT. GWR also indicates that aggradation landscape positions tend to trap or retain greater thicknesses of volcanic ash as compared to degradation landscape positions. Nonstationarity tests indicate that there are underlying soil-climate-landscape spatial processes occurring that cannot be addressed through a global model, but can be broadly accounted for using this local regression approach.

Parameter estimate surfaces were draped over a 30-m shaded relief USGS digital elevation model to assess potential linkages between estimated nonstationarity patterns and landscape features (Figure 2.4). ELE displays several “hotspots” across the landscape (Figure

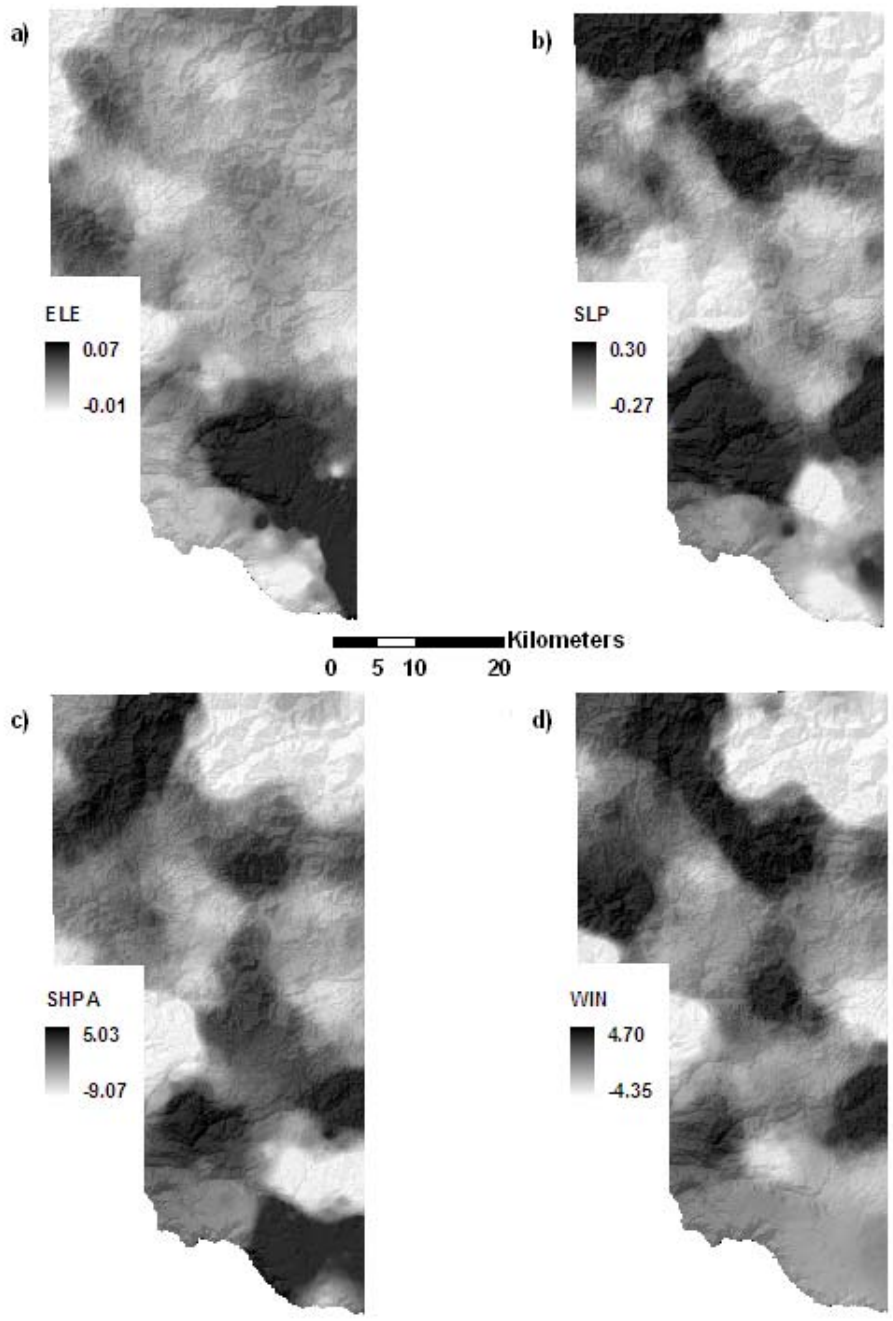

Figure 2.4. Interpolated geographically weighted regression parameter estimate surfaces from 671 observations for the independent variables a) ELE, b) SLP, c) PLCU, and d) WIN located in a forested north central Idaho landscape. Surfaces are draped over a 30-m USGS shaded relief digital elevation model.

2.4a). In the southeast sector, ELE shows a significant increase in AT. We hypothesize that this dramatic difference is due to a topoclimatic sequence that initiates adjacent to the study region. Dry, low-elevation canyons that historically would have been susceptible to considerable wind erosion and ash redistribution lie to the southwest of this "hotspot". Re-entrained volcanic ash would subsequently be transported with the northeasterly prevailing winds and deposited within the "hotspot" region of our study area.
Across the ELE parameter surface, there are pockets of positive (dark) and negative (light) influence on AT. Interestingly, the negative pockets in the northwest occur at high-elevations where our global assessment indicates we should find the thickest ash mantles. Oppositely, the positive "hotspot" in the southeast is located at low elevations, which are typically associated with thinner ash mantles in the MLR model. The positive areas to the west and northeast are more indicative of the global results. It is evident from these observations that GWR is accounting for localized topographic attributes that enhance or reduce the effect of ELE on AT.

A SLP parameter surface was included to illustrate its affect on AT, although the variation in the estimated parameter estimates was not significant (Figure 2.4b). In the northeast portion of the study area, SLP shows a negative correlation with AT. We attribute this to high precipitation in high topographic relief regions. This sector has been estimated to receive ~1500 mm of precipitation annually (Idaho State Climate Services, 2000). The combination of steep slopes (>45 percent) and high rainfall explain the negative influence of SLP. Several other zones of negative SLP parameter estimates are evident in the west and southeast portions of our study area. These sectors are dominated by steep southerly aspects and are located within or near high relief drainage basins. Consequently, these areas would tend to be

drier and more susceptible to wind and/or water erosion. The south sector shows a wide area of positive parameter estimates. Positive estimates would seem incongruous at first in this particular area, because of its high relief and dry climatic conditions. But, when WIN parameters are compared (Figure 2.4d), the trend does seem logical. WIN shows positive, or at least neutral, estimates for the same area. This result suggests that water erosion may have redistributed the volcanic ash further downslope. Thus, landscapes with steep slopes, but a larger upslope contributing area, would show thicker ash mantles in this region. An opposite trend is found in the northeast sector of the study area. Negative WIN parameter estimates in this region suggest that locations influenced by large upslope contributing areas would be less likely to have thicker deposits of volcanic ash. We interpret this finding as a function of SLP and precipitation. Steep slopes, in combination with ~1500 mm of annual precipitation, enhanced the erosion of volcanic ash downslope. Consequently, we expect to see thicker ash mantles upslope with continuous thinning to the dendritic drainage basins.

The PLCU parameter surface reflects similar spatial patterns to both SLP and WIN (Figures 2.4b,c,d). The northeast and west sectors show significantly negative parameter estimates; however, the interpretation of these negative coefficients is different for PLCU than for SLP and WIN. PLCU can have either a positive or a negative value. Positive values reflect convex surfaces; whereas, negative values indicate surface concavities. Thus, a negative parameter estimate for PLCU indicates that concavities would positively influence volcanic ash retention as opposed to convex surfaces. The positive parameter estimates found in the southeast portion of our study area indicate that volcanic ash is stable on convex surfaces. This could partially be attributable to shallow slopes and lower MAP. Volcanic ash, once established in this drier region, would not be exposed to extreme climatic and

topographic redistribution forces as found in the northern portion of our study area. Negative parameter estimates found in the northeast and west sectors would indicate that hydrologic forces increased volcanic ash erosion from convex landscape positions.

How these selected terrain attributes combine to influence volcanic ash distribution across the study area is illustrated in Figure 2.5. Using Equation 2.3, parameter surfaces were multiplied by their respective grids and summed. An output map was produced and a sub-region of the study area was selected for graphic enhancement in order to portray the effect of terrain attributes on AT. An east-west transect across the selected illustration area displays a generally increasing elevation gradient that closely follows the distribution of volcanic ash. Higher elevations typically show thicker ash mantles. The central area of the sub-region shows that wind may have re-entrained the volcanic ash in the flat, low-elevation plateau and deposited it downwind over high, forested elevations.

Slope effects can clearly be seen in the northeast sector. Slope values typically exceed 60 percent from the mountain crest to the river bottom, whereas slope does not exceed 45 percent on the southerly aspects. This result further supports our hypothesis that volcanic ash is relatively stable on slopes <45 percent. The accumulation of eroded volcanic ash into concave landscape positions is evident in the northwest sector. AT is greater in the concave positions and shows erosion from convex ridges.

A problem that arose during the modeling process can be observed in the northwest sector. Catchment basins often show ash depths >36 cm. Model validation indicates that the GWR approach can over or under-estimate AT in accumulation zones. This may be a consequence of highly variable AT observations within similar landscape positions. The local

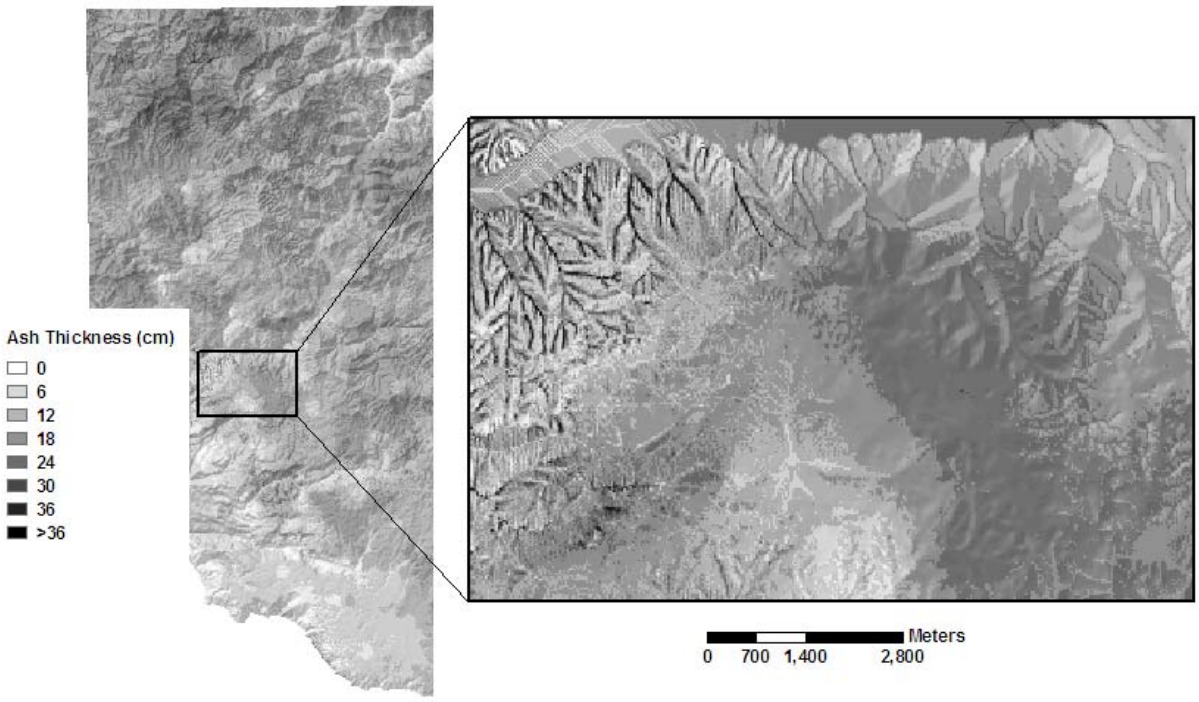

Figure 2.5. Predicted volcanic ash distribution and thickness in a forested north central Idaho landscape using geographically weighted regression.

least squares analysis approach yields the best fit to the data, but the error within the estimated values would be determined by the degree of variability in the observations.

SUMMARY

Volcanic ash distribution in forested landscapes of north Idaho is extensive. Knowledge of ash distribution patterns is important to limit any negative impact of management activities on the presence of volcanic ash. Soil surveys can provide a gross estimate of these distribution patterns; however, these estimates are often generalized across the landscape and consequently cannot provide quantitative estimates at the site-specific management scale. Therefore, it is crucial to develop an ash distribution model that can provide natural resource managers with an estimate of the volcanic ash found in their management area.

This research was conducted to meet this need. Two statistical models were sequentially developed to assess terrain attributes and their influence on the distribution of volcanic ash across the landscape. Multiple linear regression analysis found that elevation and slope were significantly correlated with ash thickness ($p = 0.05$); however, elevation accounted for >90 percent of the variance reduction. Elevation was positively correlated with ash presence, which can be ascribed primarily to wind redistribution during the droughty period following the eruption of Mt. Mazama. The silty texture of volcanic ash makes it susceptible to re-entrainment by wind and subsequent deposition downwind. Higher elevations historically had more vegetation, allowing higher elevation sites to trap and retain greater amounts of volcanic ash. Lower elevations, which were historically drier and supported less vegetation, were initially susceptible to wind erosion. Unfortunately, these relationships explained only 28 percent of the variation in ash thickness and produced a relatively high model prediction error of 14.7 cm.

Geographically weighted regression was used to determine if global relationships were masking landscape interactions at the local level. This statistical technique does not assume that parameter estimates for the independent variables are stationary across the landscape as does ordinary multiple regression analysis. Using geographically weighted regression, we found that plan curvature and wetness index, both related to deposition, were significantly correlated with volcanic ash at the local level ($p = 0.05$). Elevation was also found to be significantly nonstationary ($p = 0.05$). The effect of slope gradient, slope curvature, and wetness index on ash thickness often varied by elevation and moisture regime. Moisture-accumulating landscape positions were significantly correlated with thicker ash mantles at elevations receiving high mean annual precipitation. Conversely, convex and gentle slope landscape positions were more likely to exhibit thicker ash mantles than concave surfaces at elevations receiving low mean annual precipitation.

In conclusion, results using geographically weighted regression revealed terrain-volcanic ash thickness relationships that were masked in the ordinary multiple regression analysis. These newly quantified relationships were subsequently incorporated into an ash thickness map based on GWR model predictions. Local linear regression reduced model error by 4.3 cm over global linear regression. Natural resource managers can use this map to potentially improve their land management decision support systems.

LITERATURE CITED

Bacon, C.R. 1983. Eruptive history of Mount Mazama and Crater Lake caldera, Cascade Range, USA. J. Volcanol. Geotherm. Res. 18:57-115.

Brown, H.G., and H. Loewenstein. 1978. Predicting site productivity of mixed conifer stands in northern Idaho from soil and topographic variables. Soil Sci. Soc. Am. J. 42:967-971.

Brunsdon, C., A.S. Fotheringham, and M.E. Charlton. 1996. Geographically weighted regression: A method for exploring spatial nonstationarity. Geographical Analysis. 28:281-298.

Buol, S.W., R.J. Southard, R.C. Graham, and P.A. McDaniel. 2003. Andisols: Soils with Andic properties. *In* Soil genesis and classification. 5th ed. Iowa State Press. Ames, IA. pp. 231-241.

Busacca, A.J., H.M. Marks, and R. Rossi. 2001. Volcanic glass in soils of the Columbia Plateau, Pacific Northwest, USA. Soil Sci. Soc. Am. J. 65:161-168.

Cullen, S.J., C. Montagne, and H. Ferguson. 1991. Timber harvest trafficking and soil compaction in western Montana. Soil Sci. Soc. Am. J. 55:1416-1421.

FAO/ISRIC/ISSS. 1998. World Reference Base for Soil Resources. Food and Agricultural Organization of the United Nations, International Soil Reference and Information Centre, and International Society of Soil Science. World Soil Resources Report #84. Rome.

Florinsky, I.V., R.G. Eilers, G.R. Manning, and L.G. Fuller. 2002. Prediction of soil properties by digital terrain modelling. Environmental Modelling and Software. 17:295-311.

Fotheringham, A.S., C. Brunsdon, and M. Charlton. 2002. Geographically weighted regression: The analysis of spatially varying relationships. John Wiley and Sons, New York. 265 p.

Gardner, B. 2005. Personal communication. Soil Scientist. USDA – Natural Resources Conservation Service. Moscow, ID.

Geist, J.M., and G.S. Strickler. 1978. Physical and chemical properties of some Blue Mountain soils in northeast Oregon. USDA For. Serv. Res. Pap. PNW-236. 19 p.

Gessler, P.E., I.D. Moore, N.J. McKenzie, and P.J. Ryan. 1995. Soil-landscape modelling and spatial prediction of soil attributes. Int. J. Geographical Information Systems. 9:421-432.

GWR. 2005. Geographically weighted regression software 3.0. National Centre for Geocomputation. National University of Ireland. Maynooth, Ireland.

Hope, A. 1968. A simplified Monte Carlo significance test procedure. Journal of the Royal Statistical Society Series B. 30:582-598.

Hunter, C.R. 1988. Pedogenesis in Mazama tephra along a bioclimatic gradient in the Blue Mountains of southeastern Washington. Ph.D. Dissertation. Washington State Univ. Pullman. 128 p.

Idaho State Climate Services. 2000. Digital precipitation for Idaho: Average, monthly, and annual (1961-1990). Idaho State Climate Services. Moscow, ID.

Jenny, H. 1941. Factors of soil formation: A system of quantitative pedology. McGraw-Hill, New York. 281 p.

McBratney, A.B., M.L. Mendonca Santos, and B. Minasny. 2003. On digital soil mapping. Geoderma 117:3-52.

McDaniel, P.A., M.A. Wilson, R. Burt, D. Lammers, T.D. Thorson, C.L. McGrath, and N. Peterson. 2005. Andic soils of the Inland Pacific Northwest, USA: Properties and ecological significance. Soil Science. 170:300-311.

McKenzie, N.J., and P.J. Ryan. 1999. Spatial prediction of soil properties using environmental correlation. Geoderma. 89:67-94.

McSweeney, K., P.E. Gessler, B.K. Slater, R. D. Hammer, J.C. Bell, and G.W. Petersen. 1994. Towards a new framework for modeling the soil-landscape continuum. *In* Factors of Soil Formation: A Fiftieth Anniversary Retrospective. Soil Sci. Soc. Am. J. SSSA Special Publication 33. Madison, WI. 160 p.

Moore, I.D., R.B. Grayson, and A.R. Ladson. 1993a. Digital terrain modelling: A review of hydrological, geomorphological, and biological applications. J. Hydrol. 5:3-30.

Moore, I.D., P.E. Gessler, G.A. Nielsen, and G.A. Peterson. 1993b. Soil attribute prediction using terrain analysis. Soil Sci. Soc. Am. J. 57:443-452.

Moran, P.A.P. 1950. Notes on continuous stochastic phenomena. Biometrika. 37:17-23.

Mullineaux, D.R. 1986. Summary of pre-1980 tephra-fall deposits erupted from Mount St. Helens, Washington State, USA. Bull. Volcanol. 48:16-26.

Myers, R.H. 1990. Classical and modern regression with applications. Ed. 2. Duxbury, Pacific Grove, CA. 488 p.

Nammah, H., F.E. Larsen, D.K. McCool, R. Fritts, Jr., and M. Molnau. 1986. Mt. St. Helens volcanic ash: effect of incorporated and unincorporated ash of two particle sizes on runoff and erosion. Agric. Ecosystems Environ. 15:63-72.

Ord, J.K., and A. Getis. 1995. Local spatial autocorrelation statistics: Distributional issues and an application. Geog. Anal. 27:286-306.

Richmond, G.M., R. Fryxell, R. Neff, G.E. Neff, and P.L. Weis. 1965. The Cordilleran ice sheet of the northern Rocky Mountains and related Quaternary history of the Columbia Plateau. *In* H.E. Wright Jr. and D.G. Frey (ed.). The Quaternary of the United States. Princeton Univ. Press. Princeton, NJ. pp. 231-242.

Ruhe, R.V., and C.G. Olson. 1980. Soil welding. Soil Science. 22:66-69.

Ryan, P.J., N.J. McKenzie, D. O'Connell, A.N. Loughhead, P.M. Leppert, D. Jacquier, and L. Ashton. 2000. Integrating forest soils information across scales: spatial prediction of soil properties under Australian forests. For. Ecol. Manage. 138:139-157.

Shipley, S., and A.M. Sarna-Wojcicki. 1983. Distribution, thickness, and mass of late Pleistocene and Holocene tephra from major volcanoes in the northwestern United States: A preliminary assessment of hazards from volcanic ejecta to nuclear reactors in the Pacific Northwest. US Geol. Surv. Misc. Field Studies Map. MF-1435. Washington, DC. 27 p.

Soil Survey Staff. 1999. Soil taxonomy. A basic system of soil classification for making and interpreting soil surveys. 2nd ed. USDA – Natural Resources Conservation Service. Agricultural Handbook No. 436. U.S. Govt. Print. Office. Washington, DC.

Warkentin, B.P., and T. Maeda. 1980. Physical and mechanical characteristics of Andisols. *In* B.K.G. Theng (ed.) Soils with variable charge. Offset Publications. Palmerston North, NZ. pp. 281-301.

Warren, A. 1979. Aeolian processes. *In* I.P. Martini and W. Chesworth (ed.) Weathering,Soils, and Paleosols. Elsevier. Amsterdam. pp. 225-260.

Wilson, J.P., and J.C. Gallant. 2000. Digital terrain analysis. *In* J.P. Wilson and J.C. Gallant (ed.) Terrain Analysis: Principles and Applications. John Wiley and Sons, New York. pp. 1-27.

Zdanowicz, C.M., G.A. Zielinksi, and M.S. Germani. 1999. Mount Mazama eruption: Calendircal age verified and atmospheric impact assessed. Geology 27:621-624.

Zobel, D.B., and J.A. Antos. 1991. 1980 tephra from Mt. St. Helens: Spatial and temporal variation beneath forest canopies. Biol. Fertil. Soils. 12:60-66.

CHAPTER 3: A Geographically Weighted Regression Analysis of Douglas-fir (*Pseudotsuga menziesii* [Mirb.] Franco var. *glauca*) Site Index in North Central Idaho

PREFACE

The following chapter shifts the emphasis of the dissertation from volcanic ash modelling to Douglas-fir site index modelling. The reader will note that within the site index models proposed in Chapter 3, volcanic ash becomes an independent variable as compared to being the dependent variable in the preceding chapters. Further, several independent variables used to model volcanic ash distribution are also included as independent variables within the site index models.

A question may arise as to variable redundancy by including both the dependent variable and several independent variables from the ash model into the site index models. Variable redundancy is not an issue because the independent variables common to the ash and site index models influence the dependent variables' differently. A site index model developed with independent variables common to the volcanic ash model will not capture the independent influence of volcanic ash on site index. Thus, volcanic ash is included as an independent variable.

All chapters within this dissertation were written in journal format. Each chapter was written to the format required by the journal of choice. Format requirements for the first two chapters included expressing all units in metric. The journal format requirements for Chapter 3 included expressing units in English units. Consequently, all model statistics are expressed in inches (in), feet (ft), miles (mi), and acres (ac).

ABSTRACT

An analysis of Douglas-fir (*Pseudotsuga menziesii* [Mirb.] Franco var. *glauca*) site index (SI) was conducted in north central Idaho using two forms of linear regression: 1) standard multiple linear regression (MLR), and 2) geographically weighted regression (GWR). The hypothesis was that the GWR model would provide better estimates of SI using edaphic, topographic, and climatic predictor variables than ordinary MLR. Elevation, volcanic ash depth, slope, and aspect were significantly correlated with Douglas-fir SI ($R^2 = 0.5$). GWR accounted for an additional 28 percent of the variation in SI and reduced the error sum of squares by 54 percent. The geographically weighted parameter estimates of elevation were nonstationary, which indicates that a specific elevation can exert either a positive or negative influence on SI depending on geographic location. Residual analysis from a MLR model showed SI overestimation in the south and west of our study area. This overestimation was significantly reduced using the GWR model. GWR shows promise for future biological modelling.

INTRODUCTION

Site index (SI) is commonly accepted as an estimate of site productivity in forestlands of the Inland Northwest and beyond (Brown and Loewenstein, 1978; Corona et al., 1998; Curt et al., 2001; Green et al., 1989; Monserud, 1984; Vander Ploeg and Moore, 1989). SI, as defined by the index age and height of a specified subset of dominant trees of a given species, has been closely associated with a site's ability to support wood production (Green et al., 1989; Spurr and Barnes, 1980). The relative ease of collecting height/age measurements and the subsequent use of SI calculations in yield models has led to the development of SI curves for many of the tree species found within the Inland Northwest (Barrett, 1978; Cochran, 1979a; Cochran, 1979b; Monserud, 1984). However, field estimation of SI is often complicated by adverse effects on height growth from fire or insects and disease (Kayahara et al., 1998; McLeod and Running, 1988; Monserud, 1984). Sites may also be stocked with species other than the one of interest, or unstocked from past management activities (Kayahara et al., 1998). In these situations, estimating SI as a measure of local productivity from environmental variables would be beneficial.

However, the use of SI must be kept in context of time and definition. Different definitions on tree selection criteria are often used to estimate SI. This can lead to inconsistent and potentially biased SI estimates. Further, measurement of SI is a point estimate in time. SI estimates will change for a location once a new set of site trees are selected. Despite these shortcomings, measurement of SI does allow natural resource managers to predict one value of site productivity across the landscape.

Numerous efforts for assessing SI using soil-site factors have been studied in North America (Brown and Loewenstein, 1978; Burger and Kelting, 1999; Monserud et al., 1990;

Schoenholtz et al., 2000; Uzoh, 2001) and elsewhere (Corona et al., 1998; Curt et al., 2001; Kayahara et al., 1998; McKenney and Pedlar, 2003; Rodriguez et al., 2002; Stendahl et al., 2002; Wang and Klinka, 1996). The range in rationale and modelling methods employed in these studies is extensive, but commonalities in results do exist. Elevation, precipitation, and various measures of soil water holding capacity and soil nutrient status were commonly correlated with SI. However, many of these studies noted that interactions between environmental variables produce a spatial complexity that is difficult to capture within a statistical model.

The most common statistical method employed to estimate SI has been multiple linear regression (MLR) (Brown and Loewenstein, 1978; Curt et al., 2001; Green et al., 1989; Monserud et al., 1990). MLR assumes that each independent variable brought into a model affects the dependent variable uniformly (i.e., the assumption of stationarity) across the study area (Fotheringham et al., 2002). For example, MLR assumes that an elevation of "X" will have the same effect on "Y" (SI) at point "A" as at point "B". Hypothetically, MLR may not account for the fact that point "B" is located within a mountainous region that produces climatic conditions dissimilar to point "A". Shifts in climatic conditions may change the sign or slope of the elevation coefficient. This shift or sign change is not shared by point "A", hypothetically found in drier, less mountainous regions. Consequently, what are actually two separate elevation effects on SI are modeled within MLR as a single elevation effect. The result is an elevation coefficient with a large standard error and potentially imprecise estimates of SI. MLR is incapable of capturing the spatial complexity of landscape interactions at the local level.

Phenotypic response to genetic variation induced by local environmental conditions is an additional source of variation that is rarely captured in SI studies. Obtaining a measure of genetic effects on SI is difficult, however genetic effects on SI have been shown to contribute a significant source of variation in Douglas-fir (*Pseudotsuga menziesii* [Mirb.] Franco var. *glauca*) and lodgepole pine (*Pinus contorta* [Engelm. in Wats.] var. *latifolia*) species (Monserud and Rehfeldt, 1990). MLR analysis of SI will be unable to account for the interactive effects of local genetic and environmental influences without this measure of genetic variation. Thus, assuming that: 1) genetic variation is uniform, and 2) a suite of independent variables interact in precisely the same manner to affect SI and genetic response, regardless of geographic location, is troublesome.

Wang et al. (2005) suggested the use of nonparametric models to avoid the assumptions inherent to least-squares regression. Tree-based regression (TREE), generalized additive models (GAM), and neural network models (NNT) were advanced as alternatives because nonparametric methods do not pre-specify a relationship between SI and environmental variables. In addition, the algorithm approach to nonparametric modelling reduces the potential negative effect of collinearity within the independent variables. Monserud et al. (1990) suggested that many of the key variables used in his MLR analysis of Douglas-fir SI were not independent and were probably different measures of the same growth factors. The consequence of modelling with collinear variables as in Monserud et al. (1990) is the potential for inflating both parameter estimate variance and confidence interval bands around prediction values (Belsley et al., 1980; Wang et al., 2005). However, there are drawbacks to nonparametric modelling. Nonparametric methods can derive relationships between the independent and dependent variables that are often difficult to interpret (Breiman, 2001).

Therefore, if the primary objective is to derive biological relationships that are readily interpreted, then the data modelling approach of MLR or nonlinear regression (NLR) are the best methods.

A parametric modelling method that may: 1) provide readily interpretable biological relationships, 2) measure sources of local variation, and 3) reduce variable collinearity is a geographically weighted regression analysis (GWR). GWR as developed by Fotheringham et al., (2002), relies on a form of kernel regression within a MLR framework to develop local, as opposed to global, relationships between the dependent and independent variables. The development of local relationships facilitates an exploratory analysis of the stationarity assumption of a global MLR model. Relaxing the stationarity assumption may eliminate the need to rely on nonparametric modelling to reveal potentially complex variable interactions across geographic space. The subsequent derivation of spatial maps representing parameter estimate nonstationarity and spatial estimates of SI using the GWR method has to our knowledge never been attempted.

Therefore, the objectives of this study were to: i) assess the differences between GWR and MLR model SI estimates in a north central Idaho forest, ii) test nonstationarity of the independent variables, iii) determine if a parametric GWR analysis enhances our understanding of environmental influences on Douglas-fir SI, and iv) derive a spatial display of GWR SI estimates.

MATERIALS AND METHODS

Environmental Characteristics

Our study area is located in north central Idaho along the west slopes of the Clearwater Range and east of the Columbia Basin. This study area encompasses ~ 510,000 ac of diverse

moisture regimes, habitat types, and terrain attributes. Landscapes of this region are generally characterized as mountainous in the north and east, while the south and west is characterized as basalt plateaus/benchland incised with deep canyons. Soil parent material varies widely from metasedimentary schists and quartzites to igneous granites and basalts. Eolian deposits of loess from the Columbia Basin and volcanic ash from the eruption of Mt. Mazama are often found as intermixed mantles. Thick volcanic ash mantles are common in the north and east regions of the study area, often reaching depths >20 in. Elevation ranges from 900 ft in the southwest to >5500 ft in the north and east. Mean annual precipitation (MAP) roughly follows the elevational gradient, with <25 in MAP in the southwest and >60 in to the northeast (Idaho State Climate Services, 2000). Ponderosa pine (*Pinus ponderosa* Dougl.) and Douglas-fir habitat types dominate the southern regions of the study area. Western redcedar (*Thuja plicata* Donn) and Western hemlock (*Tsuga heterophylla* [Raf.] Sarg.) are found in the warmer, moist upland regions; with Subalpine fir (*Abies lasiocarpa* [Hook.] Nutt.) and Mountain hemlock (*Tsuga mertensiana* [Bong.] Carr.) predominant in the colder, higher elevations (Cooper et al., 1991). Douglas-fir as a conifer species has a wide geographic distribution and can be found intermixed with other Inland Northwest tree species throughout the study area and is a good “litmus test” species for site productivity in the region.

Data Collection and Sources

SI measurements were obtained from two sources: 1) 245 observations from the Natural Resource Conservation Service (NRCS) ID-612 ecological site inventory database, and 2) 45 observations from field measurements collected by the authors (Figure 3.1). SI values were based on the average age and height of three to five dominant site trees, and

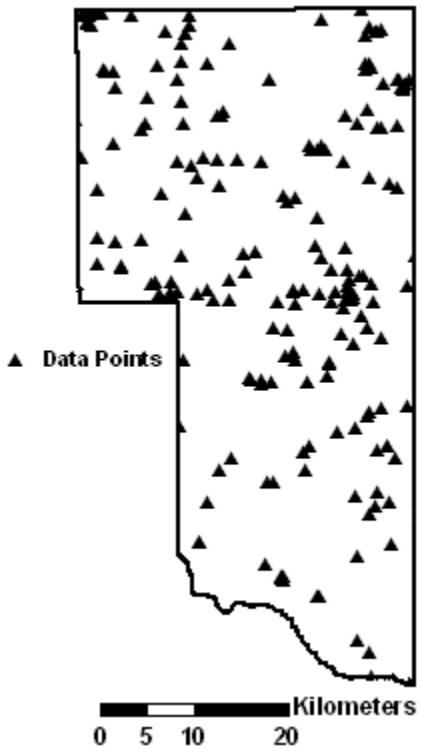

Figure 3.1. Distribution of 290 Douglas-fir site index observations in a north central Idaho landscape.

calculated from equations developed by Monserud (1985). Trees that showed defect or growth ring suppression were not sampled.

Volcanic ash thickness (AT) and total soil depths (A+B horizons, SDEP) were obtained either from soil profile description forms accompanying the 245 ecological site inventory records or through soil auguring on the additional 45 field plots. Field plot size was based on NRCS soil survey sampling protocol, which allows plot size to vary depending on the landscape characteristics inherent to a soil profile description. For the 45 field plots, soil depths were based on the average depth of three randomly distributed soil cores in the sampling area. Geologic bedrock parent material to the formation level was obtained for all 290 sites by plotting X,Y coordinates over digital 7.5 min United States Geological Survey (USGS) geology quadrangles. Geochemistry values for each formation were obtained from a database compiled from Idaho Geological Survey (IGS) and USGS rock samples (Garrison-Johnston et al., 2003). The weathering potential index (WPI) for each formation's geochemistry composition was subsequently calculated using the following modified form of Reiche's WPI equation (Garrison-Johnston et al., 2003; Reiche, 1943):

$$WPI = \frac{100 \text{ x moles}(Na_2O + K_2O + MgO + CaO)}{\text{moles}(Na_2O + K_2O + MgO + CaO + SiO_2 + Al_2O_3 + Fe_2O_3)} \qquad \text{[Eq. 3.1]}$$

WPI values are indicative of the potential plant available nutrient pools and the rapidity to which rocks will weather to form soil. Rocks with high WPI values suggest a greater supply of plant essential cations; conversely, rocks with low WPI values suggest lower weathering potential and less plant available nutrients.

Estimates of MAP were obtained from a 1:250,000-scale isohyetal precipitation map of Idaho (Idaho State Climate Services, 2000). The primary terrain attributes, elevation (ELE),

slope (SLP), and aspect (ASP) were derived from a USGS 30-m digital elevation model (DEM). Compound terrain attributes that measured plan and profile slope curvature (PLCU, PRCU), wetness index (WIN) and slope-aspect interactions (SLPCASP, SLPSASP) were computed from the USGS 30-m DEM using grid algebra in a geographic information system (GIS) (Table 3.1).

Statistical Analyses

GWR was used to estimate Douglas-fir SI as a function of environmental variables (Table 3.1). This modelling approach involved several separate statistical analyses to determine: 1) the global significance of independent variables and initial global MLR model, 2) the reduction of model error through local MLR, and 3) nonstationarity within the parameter estimates. The first analysis was conducted using the ordinary least squares regression model (REG) STEPWISE procedure in version 9.1 of SAS (SAS Institute, 1990). Variable significance was based on estimated *t*-values for the parameters and their associated standard errors. We used a significance level of 0.1 to retain independent variables in the model. Model variables were assumed measured without error. However, this assumption was taken with caution, because of the reliance on: 1) data collected over a period of time by different field foresters, and 2) DEM-derived data with an accuracy of 30-m. Measurement error can lead to an inflated model error term, thus underestimating the *F*-statistic. This may lead to the elimination of variables that may have been significant if measured without error. Consequently, it cannot be assumed that insignificant independent variables have no effect on SI, because of potential observation and/or imputed error during data collection.

An MLR equation was developed from the selected independent variables of the following general form:

Table 3.1. Summary of collected site and stand characteristics for 290 observations located in a north central Idaho landscape.

Site Variables	Code	Min.	Mean	Max.	Transformations (code)
Site Index (ft, Base Age 50)	**SI**	**43**	**84**	**119**	
Soil Morphological					
Ash Thickness (in)	**AT**	**0**	**12**	**26**	**log (LAT)**
A+B Soil Depth (in)	**SDEP**	**6**	**50**	**100**	
Parent Material					
Weathering Potential Index†	**WPI**	**4.17**		**22.94**	
Terrain					
Elevation (ft)	**ELE**	**1293**	**3303**	**5364**	**square (ELE2)**
Slope (%)	**SLP**	**0**	**37**	**68**	**log (LSLP), tan (TSLP)**
Aspect (°)	**ASP**				
Compound Terrain Attributes					
Plan Curvature	**PLCU**	**-4.85**	**0.02**	**6.96**	
Profile Curvature	**PRCU**	**-6.17**	**-0.01**	**4.37**	
TSLP*cos(ASP)	**SLPCASP**	**-1.01**	**-0.07**	**1.01**	
TSLP*sin(ASP)	**SLPSASP**	**-1.01**	**0.02**	**1.01**	
Wetness Index	**WIN**	**6.69**	**8.96**	**14.82**	
Climate					
Mean Annual Precipitation (in)	**MAP**	**25**	**38**	**60**	

† Modified Reiche (1943) equation.

$$SI_{(i)} = \beta_0 + \beta_1 X_{1(i)} + \beta_2 X_{2(i)} + \ldots + \beta_k X_{k(n)} + \varepsilon_i \quad \text{[Eq. 3.2]}$$

where $SI_{(i)}$ = estimated site index at observed point *i*; $\beta_k = k^{th}$ global parameter estimate; $X_{k(n)} = k^{th}$ independent variable value at the n^{th} location; and ε_i = model error at point *i*. Overall model fit and performance were assessed through the adjusted coefficient of determination (R^2_A) and root mean square error (RMSE).

The second analysis was performed to determine if a GWR model derived from the locally computed parameter estimates outperformed the global MLR model. Version 3.0 of GWR software was used (GWR, 2005). GWR utilized a form of kernel regression and MLR to build a model that can be generally stated as follows:

$$SI_{(i)} = \beta_{0(i)} + \beta_{1(i)} X_{1(i)} + \beta_{2(i)} X_{2(i)} + \ldots + \beta_{k(n)} X_{k(n)} + \varepsilon_i \quad \text{[Eq. 3.3]}$$

where $SI_{(i)}$ = estimated site index at observed location *i;* $\beta_{k(n)} = k^{th}$ local parameter estimate at the n^{th} location; $X_{k(n)} = k^{th}$ independent variable value at the n^{th} location; and ε_i = model error at location *i*.

The loose similarity to kernel regression arises from the development of a search neighborhood (i.e., bandwidth) used to derive local parameter estimates. Bandwidths can be considered as smoothing functions of the local parameter estimates. Caution must be exercised when deriving bandwidths. Large bandwidths can oversmooth the parameters, reducing the ability to capture local variability in the independent variables. Oppositely, small bandwidths produce parameter estimates with large local variation, reducing the ability to assess trends within the data (Fotheringham et al., 2002).

The choice of an optimal bandwidth can be determined using several methods: 1) cross-validation (CV), 2) Akaike's Information Criteria (AIC), and 3) user-defined. CV and AIC bandwidth selection is primarily used with datasets where there is no prior justification of a bandwidth or knowledge of the dataset is minimal. The objective of these methods is to find a bandwidth that minimizes the CV or AIC score. In situations where an analyst is familiar with a dataset or has previous knowledge of an acceptable bandwidth, a user-defined bandwidth is optimal. User-defined bandwidths can be derived through either an adaptive or fixed approach.

Adaptive bandwidths are best suited for datasets with irregular sampling intervals. The adaptive technique relies on either an absolute or relative number of observations to be included within the localized regression. Consequently, the bandwidth will vary depending on the concentration of observations. In areas with high concentration of data points, bandwidths will decrease. Oppositely, in areas with a low density of observations, bandwidths are allowed to expand to meet the defined percentage or number of observations.

A fixed bandwidth is based on a defined diameter of a circular search neighborhood. The diameter scalar units are the same as the location variables. Selection of this bandwidth diameter can be specified in one of two ways: 1) theoretically defined, or 2) minimization of the model's AIC score (Fotheringham et al., 2002). Theoretically defined bandwidths can be associated with a previously assessed spatial function within the dependent variable. Bandwidth selection by AIC score minimization provides an alternative if a dependent variable's spatial function is unknown.

The geographic weighting occurs once a regression model (Gaussian, Logistic, or Poisson), bandwidth, and kernel type have been selected. Local parameter estimates are

derived from the regression of data points within a kernel's bandwidth. The influence of a data point on the local parameter estimate is weighted based on the geographic distance from the regression point. Locations nearer the regression point of interest are weighted heavier than those points located farther away (Fotheringham et al., 2002). This differs from weighted least-squares analysis (WLS), which attempts to address local variance by adjusting the parameter estimates by a matrix of error variances (Myers, 1990).

For our analysis, a Gaussian model with a user-defined, fixed bandwidth kernel was applied to the data. The fixed bandwidth kernel was determined by iteratively applying a stepped distance to the observed data until the optimum distance was achieved. The optimum distance was defined as the point at which: 1) the AIC score and RMSE were minimized, and 2) the R^2_A value was maximized.

Once a local model was built, GWR computed an *F*-statistic to determine if the consumption of additional *df* in the local model was offset by the additionally explained residual sum of squares. The upper 0.1 percentile of the *F*-distribution was chosen as the significance level for our study. In addition to an *F*-test, an AIC score comparison was performed between the local and global models. The AIC statistic measures the information distance between model distribution *g* and the true distribution *f*. A comparison of this quantity between differing models $g_1, \ldots, g_n$, can be used to assess which model more closely represents the true distribution. Relative improvements of the AIC criteria >3 are associated with genuine differences between the global and local models. AIC differences <3 in the local model could be attributable to sampling error and are therefore not considered to be a significant improvement (Fotheringham et al., 2002). For our study, both the *F*-statistic

and AIC minimization were used to assess the significance of the localized GWR model. Overall model fit and prediction was assessed through the R^2_A and RMSE statistics.

The parameter estimates obtained in the initial global MLR model are assumed to be stationary across a study area. GWR computed a Monte Carlo significance test on the locally derived parameter estimates to assess if this assumption was valid (Hope, 1968). The Monte Carlo test calculated the observed variance of local parameter estimates, which was then compared against 99 simulated sets of variances obtained through randomizations of the observed data. Probability values were then computed for each variable's parameter estimates. We used a significance level of 0.05 to determine if the parameter estimates met the stationarity assumption. Nonstationary parameter estimates were spatially interpolated using a deterministic inverse distance weighted function (IDW) to assess patterns across our study area.

Once a localized regression model was fit that met the overall model and parameter significance requirements, parameter estimate surfaces for the selected independent variables were interpolated using the IDW function. Interpolated parameter estimates and their respective raster grids were combined using Equation 3.3. A spatial display of locally estimated SI was subsequently generated using GIS.

RESULTS

Environmental Characteristics

Volcanic ash was significantly related to SI (p <0.0001). The logarithm of ash thickness (LAT) showed a curvilinear increase in SI with increasing AT (Figure 3.2). The inflection point of the curve occurs at approximately three inches of ash depth. As ash thickness increases, its influence on SI increases toward an asymptote that was not defined within the

range of our data. SDEP showed no significant effect on SI (p >0.1) and was subsequently dropped from the analysis. Bedrock geology was classed into 12 WPI categories ranging in value from 4.2 to 22.9. Only three WPI categories showed significant effect on SI: anorthosite (20.7), calc-silicate quartzite (18.3), and gneiss (9.1). Unfortunately,

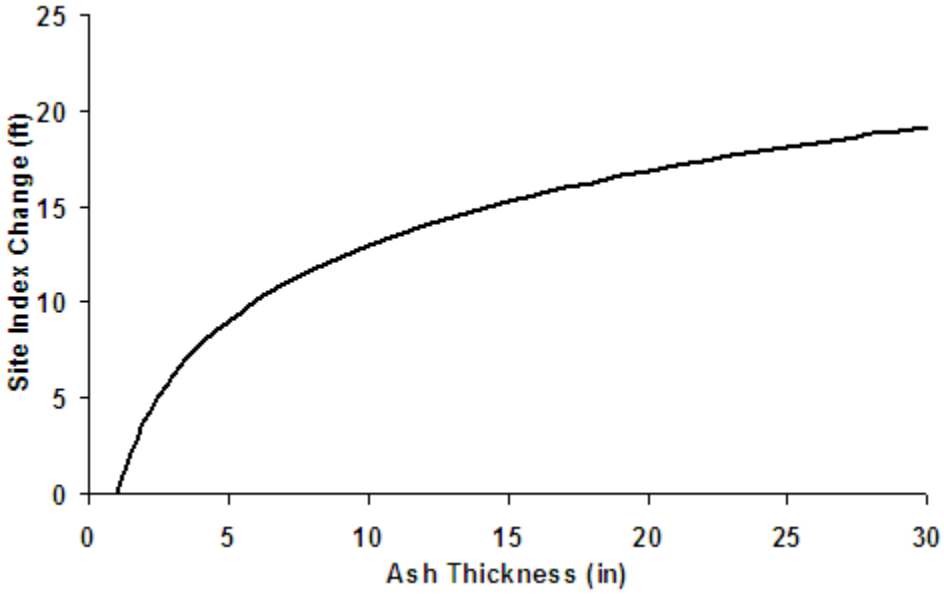

Figure 3.2. Partial regression analysis of the logarithmic effect of volcanic ash on Douglas-fir site index in north central Idaho. Response was derived holding all other model variables at their means.

these geologic formations had limited distribution across our study area and were confounded with areas of high MAP. Consequently, WPI was dropped from the analysis.

The topographic feature showing the strongest relation to SI was the square of elevation (ELE2) (p <0.0001). ELE2 showed a significant curvilinear reduction in SI with increasing elevation (Figure 3.3). SLP and ASP effects on SI were assessed using Stage's (1976) transformation. The combined effect of SLP and ASP was determined by multiplying the cosine and sine of ASP by the tangent of SLP (SLPCASP and SLPSASP, respectively). SLPCASP was marginally insignificant (p = 0.1034); however, SLPSASP showed significant influence on SI (p <0.05). To maintain the integrity of Stage's (1976) transformation equation, SLPCASP was retained in subsequent models. Independently, the logarithm of SLP (LSLP) showed significant, positive influence on SI (p <0.05). Figure 3.4 suggests that an increasing slope gradient on southwest facing slopes is optimal for Douglas-fir height growth. Topographic soil moisture indices, PRCU, PLCU, and WIN, showed no significant effect on SI (p <0.1) and were subsequently dropped from further consideration.

MAP showed marginal significance in the presence of other independent variables (p <0.1). Interestingly, MAP alone failed to account for any significant variation in SI. We attribute this result to the scale at which MAP was derived. At 1:250,000, the estimates were too crude to capture variation in SI across our geographic study area. Indeed, a binary variable dividing MAP into two categories, MAP >30 or ≤30 in, showed the most promise

for SI prediction. We removed MAP from further analysis to avoid introducing a source of error due to variable scale differences.

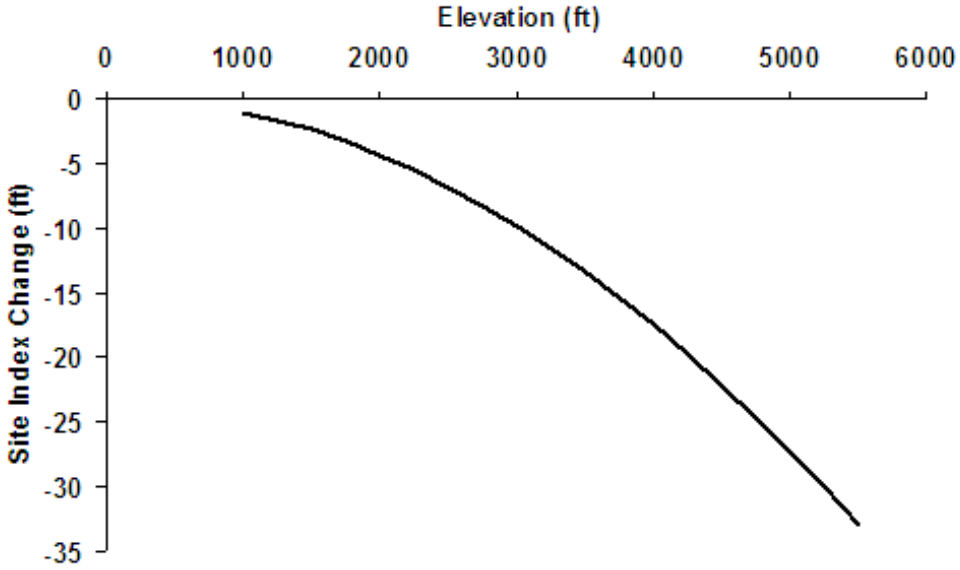

Figure 3.3. Partial regression analysis of the square effect of elevation on Douglas-fir site index in north central Idaho. Global response was derived holding all other model variables at their means.

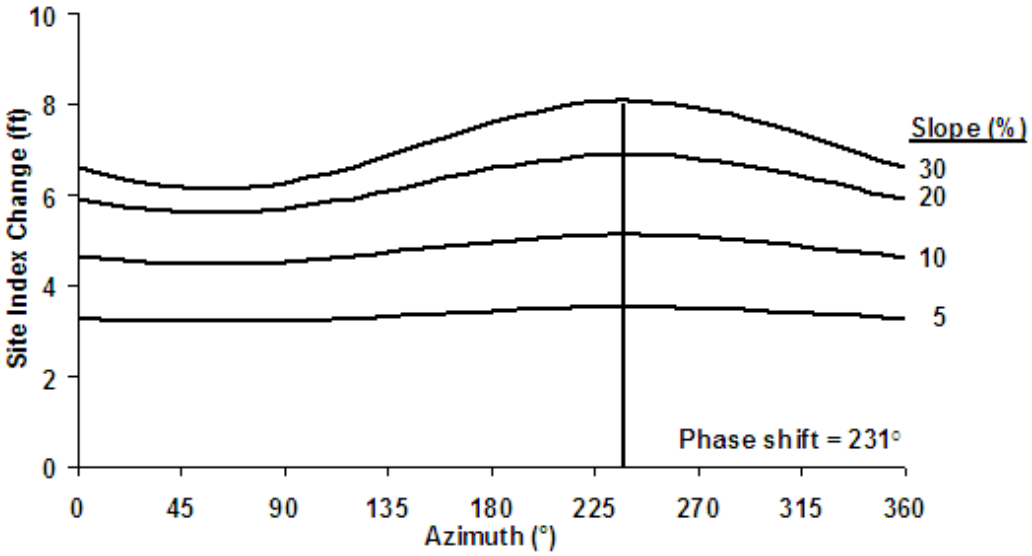

Figure 3.4. Partial regression analysis of the slope-aspect interaction effect on Douglas-fir site index in north central Idaho. The phase shift was calculated using the Stage (1976) equation.

Multiple Linear Regression Modelling

A MLR analysis was performed to determine the ability of a global regression model to estimate SI. Given the relationships described above, a MLR model was developed using predictor variables LAT, ELE2, LSLP, SLPCASP, and SLPSASP as follows:

$$SI_{(i)} = 75.6 + 13.0\ (LAT) - 0.0000011\ (ELE2) + 4.8\ (LSLP) - 2.04\ (SLPCASP) + 2.49\ (SLPSASP) \quad \text{[Eq. 3.4]}$$

where $SI_{(i)}$ is estimated site index (total height (ft) at base age 50 years at breast height) at location *i*, LAT is the log of volcanic ash thickness (in), ELE2 is the square of elevation (ft), LSLP is the log of SLP (%), SLPCASP is the tangent of SLP multiplied by the cosine of ASP (°), and SLPSASP is the tangent of SLP multiplied by the sine of ASP. The model accounted for 22 percent of the variation and had a RMSE of 11.5 ft (Table 3.2). The AIC score for this model was 2247.

Equation 3.4 was implemented in a GIS using raster grids of the model variables. Figure 3.5a shows a spatial display of classed SI values across the study area. Based on equation 3.4, SI was low in the south, southwest, and north. High SI was predicted for a relatively narrow band progressing from the west to the northeast. Average SI was predicted primarily in the east and northwest portions of the study area. However, an interpolated residuals map shows a high degree of model error throughout the study area (Figure 3.5b). The MLR model overestimates SI across a large portion of the south and west. Underestimates of SI were confined to smaller geographic areas.

Table 3.2. Fit and precision statistics for multiple linear regression (MLR) and geographically weighted regression (GWR) Douglas-fir site index prediction models for a north central Idaho landscape.

Regression Model	RMSE	R^2	Adjusted R^2	AIC
MLR	**11.5**	**0.23**	**0.22**	**2247**
GWR	**9.2**	**0.64**	**0.50**	**2240**
GWR Improvement	**2.3**	**0.41**	**0.28**	**7**

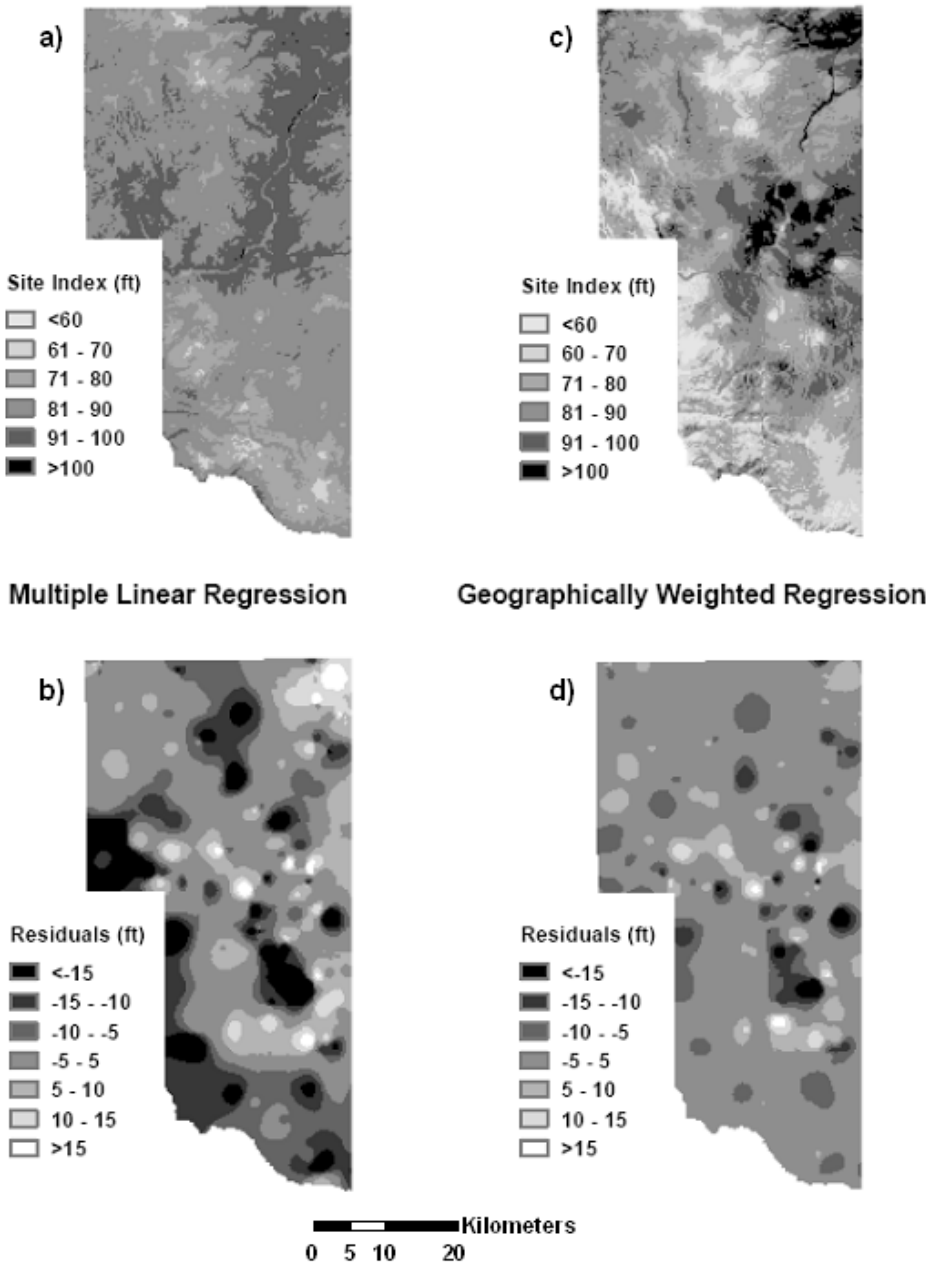

Figure 3.5. a) Spatial analysis of derived Douglas-fir site index estimates from a multiple linear regression model for a north central Idaho landscape; b) Residual analysis for the multiple regression site index model; c) Spatial analysis of derived Douglas-fir site index estimates from a geographically weighted regression model for a north central Idaho landscape; d) Residual analysis for the geographically weighted regression site index model.

Geographically Weighted Regression Modelling

An incremental approach was used to determine a bandwidth that minimized the AIC score while maintaining a low RMSE and high R^2_A. A bandwidth of ~ 3.5 mi was computed using the North American Datum (NAD) 1927, Universal Transverse Mercator (UTM) coordinates of the observation points. This bandwidth resulted in an AIC score of 2240, a net reduction of seven points over the global MLR model. The *F*-statistic, which compares the reduction of residual sum of squares between the MLR and GWR models, was found to be significant (p <0.05) (Table 3.3). Model fit and precision estimates indicate that the GWR model explains an additional 28 percent of variation in SI and reduces the MLR model error by 2.3 ft (Table 3.2). These statistics suggest that the localized approach of GWR modelling significantly improves SI estimates compared to a global model.

Spatial nonstationarity of the parameter estimates was calculated for each of the independent variables. A Monte Carlo simulation showed that only ELE2 parameter estimates were significantly nonstationary across the study area (Table 3.4). The local ELE2 parameter estimates were classed by quantile into five categories to visually assess the spatial nonstationarity (Figure 3.6). ELE2 shows positive parameter estimates primarily in the south and west, and negative estimates grading to the north.

Given the model improvement by GWR, a spatial map of SI was generated using the locally derived parameter estimates of LAT, ELE2, LSLP, SLPCASP, and SLPSASP. The specific model is:

$$SI_{(i)} = \beta_{0i}\ (\text{Intercept}) + \beta_{1i}\ (\text{LAT}) + \beta_{2i}\ (\text{ELE2}) + \beta_{3i}\ (\text{LSLP}) + \beta_{4i}\ (\text{SLPCASP}) + \beta_{5i}\ (\text{SLPSASP}) \quad \text{[Eq. 3.5]}$$

Table 3.3. Analysis of variance for multiple linear regression (MLR) and geographically weighted regression (GWR) Douglas-fir site index models for a north central Idaho landscape.

Source	SS	DF	MS	F
MLR Residuals	**37501**	**6**		
GWR Improvement	**19908**	**74.19**	**268.35**	
GWR Residuals	**17593**	**209.81**	**83.85**	**3.2****

Table 3.4. Summary of geographically weighted regression parameter estimates and their significance test for parameter nonstationarity for a north central Idaho dataset.

Parameter	Min.	Lower Quartile	Median	Upper Quartile	Max.	Monte Carlo *p*-value
LAT	**-11.90**	**2.98**	**9.08**	**17.09**	**34.97**	**0.10**
ELE2	**-0.000002**	**-0.000001**	**-0.000001**	**0.000001**	**0.000003**	**<0.01*****
LSLP	**-32.75**	**-3.77**	**1.76**	**7.94**	**19.66**	**0.10**
SLPCASP	**-29.19**	**-5.36**	**-1.15**	**2.46**	**5.63**	**0.12**
SLPSASP	**-14.71**	**1.07**	**2.73**	**4.93**	**24.51**	**0.06**

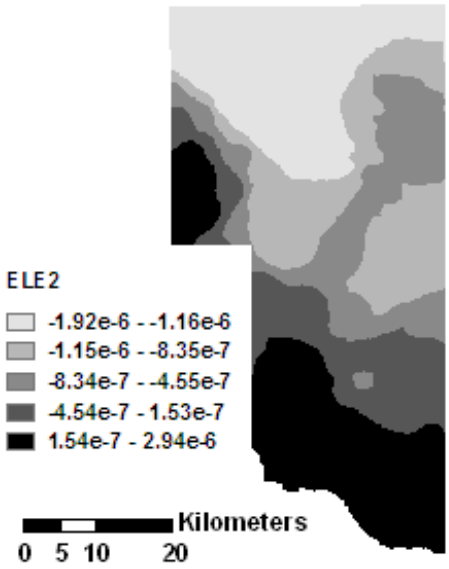

Figure 3.6. Spatial analysis of locally derived, nonstationary parameter estimates for the square of elevation in a north central Idaho landscape.

where $SI_{(i)}$ is estimated site index (total height (ft) at base age 50 years at breast height) at location *i*, $\beta_{(1\text{-}5)i}$ are the interpolated parameter estimates for the independent variables at location *i,* LAT is the log of volcanic ash thickness (in), ELE2 is the square of elevation (ft), LSLP is the log of SLP (percent), SLPCASP is the tangent of SLP multiplied by the cosine of ASP (°), and SLPSASP is the tangent of SLP multiplied by the sine of ASP.

Equation 3.5 was implemented in a GIS using raster grids of the model variables and parameter estimates. Figure 3.5c shows a spatial display of classed SI values across the study area. GWR derived SI shows much finer detail than the MLR model (Figure 3.5c). The local model captures similar spatial trends as the MLR model, but GWR accentuates the local environmental influences on SI. Broadly, GWR SI values are low in the south, southwest, and north. High GWR SI values are found in the east and northeast. Importantly, GWR estimates of SI in the west and southwest are much lower than those estimated by MLR. Interpolated residuals for GWR show a large reduction in overestimated SI values within these two regions compared to the MLR residual map (Figure 3.5b,d). On the whole, GWR estimates produced a large reduction in model error across the entire study area.

DISCUSSION

Environmental Characteristics

The influence of volcanic ash on Douglas-fir SI was found to be greater in our study area than shown in previous regional analyses (Brown and Loewenstein, 1978; Monserud et al., 1990). Monserud et al. (1990) noted that volcanic ash, as measured by chroma of the B horizon, slightly improved model standard error. In the presence of elevation and habitat series however, volcanic ash was insignificant in their analysis. Their results are surprising because it has been shown that elevation and habitat series are highly correlated with the

presence of volcanic ash in north Idaho (Kimsey et al., 2006; Steele et al., 1981). Brown and Loewenstein (1978) found a positive linear relationship between AT and SI; however, their model showed only a 2.5 ft increase in SI at 50 yrs, given a mean AT of 16.5 in. At the same AT, our data show a 15.8 ft increase in SI (Figure 3.2). In addition, our data suggest that ash thicknesses eventually reach an asymptote as opposed to the linear effect shown in Brown and Loewenstein (1978). This significant difference in ash influence on SI is probably attributable to dataset size and scope. Our dataset was an order of a magnitude larger (32 vs. 290 observations) and we selected a much smaller geographic area to study.

The strong correlation of volcanic ash with SI is primarily attributable to its high water holding capacity. A common misperception of volcanic ash soils is that they are relatively high in plant essential nutrients. However, soil nutrients are minimal as volcanic ash is primarily composed of silicon and aluminum (Dahlgren et al., 1993). It is the physical characteristics of volcanic ash that allow soils to retain a greater amount of plant available water. Soil moisture retention is critical to buffer plant communities against drought stress in the dry summer months of the Inland Northwest (McDaniel et al., 2005).

Elevation is strongly related to air temperature, precipitation, and length of growing season (Brown and Loewenstein, 1978; Curt et al., 2001; Monserud et al., 1990). Globally, elevation showed a strong negative relationship with SI (Figure 3.3). The square effect of elevation indicates that SI is increasingly reduced at higher elevations. The negative relationship observed in our data is probably due to colder temperatures at high elevations, thus reducing the length of growing season for Douglas-fir.

Locally, elevation showed significant non-stationarity (Figure 3.6). This indicates that SI responds differently to an elevation depending on its geographic location. For example, an

elevation in the southern portion of our study area exerts a positive influence on SI, whereas, in the north, that same elevation exerts a negative influence. We attribute this non-stationarity to the topography of the region. Low elevation basalt plateaus and mountain ranges dominate the southern portions of our study area. The Clearwater mountain range dominates the topography to the north and east, which consists of high mountain ridges and deep, incised valleys. These highland valleys often have the same elevation as the basalt plateaus to the south, but the climatic conditions within these valleys are often influenced by the surrounding mountain ranges. Consequently, the harsher winters and cooler summer temperatures of the mountain valleys shorten the growing season compared to similar elevations in the south.

The effect of aspect on SI was counterintuitive to our original hypothesis that northeast-facing slopes would be more productive (Figure 3.4). We assumed that northeast aspects would show higher SI because of reduced soil moisture evaporation and lower needle evapotranspiration. Indeed, SI analyses of western white pine (*Pinus monticola* Dougl.) and red oak (*Quercus rubra* L.) show higher SI on northeast aspects (Graney, 1977; Stage, 1976). However, our data show that a phase shift of 231° is optimal for Douglas-fir SI. This optimal shift suggests that the benefit of increased exposure to solar radiation is greater (i.e., a longer growing season) than the potential reduction in available soil moisture.

An alternative explanation to the observed phase shift is that the data could be masking potential elevation interactions. Phase shifts may not be constant across elevational gradients. Roise and Betters (1981) suggest that at higher, colder elevations, phase shifts may indicate optimal growth on aspects that would be suboptimal at lower, drier elevations. Our aspect data may be skewed towards more observations at the higher elevations, thereby masking

lower elevation interactions. This observation may be supported by the local non-stationarity analysis performed on the slope-aspect interaction terms (Table 3.4). The sine function of aspect shows a *p*-value of 0.06, which is only marginally insignificant. Indeed, during bandwidth selection, this variable often shifted to being significantly nonstationary. Such instability in the parameter estimates indicates that there are interactions occurring that are not being addressed by traditional statistical analyses. Additional research is necessary to address the potential of elevational influences on slope-aspect model terms.

The positive influence of slope on SI is probably attributable to soil aeration and drainage. Steeper slopes will drain more rapidly and provide a better pore ratio of air and water. Slope differences may also proxy for soil differences across our region. Many of the soils found on slopes <10 percent in the south and west have loessal soil deposits over basalt residuum. These soils have been shown to form fragipans that reduce soil aeration by severely impeding the flow of water through the soil profile during the wet spring months (McDaniel et al., 2001; Rockefeller et al., 2004). Coarser-textured soils derived from granite and metasedimentary rocks are most commonly found in the mountainous region of our study area. The combination of steeper slopes and coarser soil textures reduce the potential of poor soil drainage.

Multiple Linear Regression Modelling

A MLR model R^2_A of 0.22 and a RMSE of 11.5 ft was unexpected given the large dataset and relatively small geographic setting of our study area. Other studies using MLR to predict SI from environmental variables showed R^2_A values ranging from 0.4 to >0.7, and model errors rarely exceeding 7 ft (Brown and Loewenstein, 1978; Corona et al., 1998; Curt et al.,

2001). Monserud et al. (1990) achieved an R^2_A 0.42 and a model error of 10.9 ft with less than half the observations available in our dataset.

The low precision and fit of our MLR model may result from variable selection. Budget constraints focused our attention on variables that were: 1) inexpensive to obtain without requiring intensive field and laboratory sampling, and 2) easily modelled across geographic space. These constraints prevented an in-depth analysis of important soil characteristics, such as mineralizable nitrogen and cation exchange capacity that have been shown to influence Douglas-fir SI (Brown and Loewenstein, 1978; Kabzems and Klinka, 1987). These findings suggest that large datasets in small geographic areas do not necessarily translate to improved global regression models.

Geographically Weighted Regression Modelling

It became evident from the MLR analysis that the global approach to SI modelling was deficient. Monserud et al. (1990) states that in many soil-site relationship studies there are too many factors interacting and varying across the landscape to find significant relationships. Broadfoot (1969) noted that soil-site relations to SI are often found to be significant within small geographic areas, but these relationships could not be generalized to larger geographic areas. Such observations require a reassessment of the statistical approaches used to model natural systems, a reassessment that is beyond the scope of this paper.

The application of a GWR model to our data showed a significant improvement in capturing this local variation by reducing the MLR sum of square errors by 54 percent (Table 3.3). GWR accounted for an additional 28 percent of variation and reduced model error by 2.3 ft (Table 3.2). These results place this model within the range of precision observed in

other SI studies (Curt, 1999; Kayahara et al., 1998; McKenney and Pedlar, 2003; Monserud et al., 1990). However, our results are based entirely from field observed or DEM-derived attributes and are not reliant on expensive and time-consuming soil analyses. Many of the cited soil-site studies utilized soil chemical and physical analyses to predict SI. Such variables may improve estimates of SI, but they are difficult to obtain and model spatially.

The spatial pattern of SI in the GWR model shows very high values in the eastern portion the study area (Figure 3.4c). This area coincides with deep ash caps and mid-elevation landscapes, suggesting that elevation zones near 3,000 ft with significant ash caps are optimal for Douglas-fir growth. GWR also captures more effectively negative topographic effects in the north and southwest. These regions are characterized by colder, higher elevations and drier, lower elevation landscapes, respectively. Growth reduction is driven by shorter growing seasons in the north, and low plant available moisture in the southern portion of the study area.

GWR was found to combine the ease of modelling and interpretability of results found in global MLR analyses, with an ability to assess highly localized variable interactions that are typically only analyzed using nonparametric statistics. Our findings suggest that GWR is a good compromise between global parametric models and nonparametric analyses such as TREE, GAM, or NNT. Nonparametric statistics may yield more accurate predictions; however, natural resource managers need interpretations on why patterns exist, which can be difficult to obtain in nonparametric analyses.

GWR is also useful because it produces a seamless interaction with GIS platforms. GWR results, such as local parameter estimates, predictions, residuals, and parameter/model significance tests, can be quickly displayed spatially. Spatial displays of these statistics

enabled us to assess geographic “hotspots” in the data that would have been entirely missed in a global analysis. These “hotspots” can then be selected for further in-depth analysis to determine the mechanistic relationships producing the patterns uncovered by GWR.

The utility of GWR promises to add to the statistical modelling discussion as described by Breiman (2001). GWR, although firmly in the camp of data modelling, seems to straddle the divide between the data (MLR, NLIN) and algorithm (TREE, GAM, NNT) modelling cultures. For purists in either statistical camp this may result in questionable statistics and assumptions, but in our assessment, GWR promises to be a useful tool for developing much-needed site–forest productivity relationships regardless of spatial extent.

SUMMARY

This study’s findings indicate that Douglas-fir site index is strongly related to elevation, volcanic ash depth, slope, and aspect. Elevation was shown to be negatively associated with sit index. However, parameter estimates for elevation were nonstationary. This means that overall, colder temperatures at higher elevations shorten the length of growing season. But, our data also indicate that this elevation effect is tempered by geographic location. The same elevation in the southern portion of our study area that exerts a positive influence on tree growth has the opposite effect in the north. We attribute this shift to the topographic and climatic differences between the two portions of our study area.

Volcanic ash thickness and slope are positively correlated with site index and were stationary in their parameters. The presence of volcanic ash increases a residual soil’s ability to retain moisture. Soil moisture retention buffers Douglas-fir from drought stress during the dry summer months. Slope is primarily associated with enhanced soil drainage, but may also increase solar radiation by providing topographic relief. Douglas-fir requires warm

temperatures for optimum growth, which can only be provided through exposure to solar radiation. Aspect and its interaction with slope show that the warm, southwest quadrant is optimal; however, there is some evidence from our data that this relationship may be nonstationary.

Geographically weighted regression significantly increases model fit and precision. An additional 28 percent of the variation and 54 percent of the sum of square errors are explained when compared to a multiple linear regression model. Residual analysis of geographically weighted regression site index estimates show a large reduction in overestimated values compared to ordinary linear regression residuals. Spatial displays of geographically weighted site index estimates show greater detail than a typical regression analysis and can be used to propose future research to determine the mechanistic rationale for landscape patterns. Geographically weighted regression shows promise in future biological modelling.

LITERATURE CITED

Barrett, J.W. 1978. Height growth and site index curves for managed, even-aged stands of ponderosa pine in the Pacific Northwest. USDA For. Serv. Res. Pap. PNW-232. 14 p.

Belsley, D.A., E. Kuh, and R.E. Welsch. 1980. Regression diagnostics: Identifying influential data and sources of collinearity. John Wiley & Sons Inc., New York. 292 p.

Breiman, L. 2001. Statistical modeling: The two cultures. Statist. Sci. 16:199-231.

Broadfoot, W.M. 1969. Problems in relating soil to site index for southern hardwoods. For. Sci. 15:354-364.

Brown, H.G., and H. Loewenstein. 1978. Predicting site productivity of mixed conifer stands in northern Idaho from soil and topographic variables. Soil Sci. Soc. Am. J. 42:967-971.

Burger, J. A., and D.L. Kelting. 1999. Using soil quality indicators to assess forest stand management. Forest Ecol. Manage. 122:155-166.

Cochran, P.H. 1979a. Site index and height growth curves for managed, even-aged stands of Douglas-fir east of the Cascades in Oregon and Washington. USDA For. Serv. Res. Pap. PNW-251. 16 p.

Cochran, P.H. 1979b. Site index and height growth curves for managed, even-aged stands of white or grand fir east of the Cascades in Oregon and Washington. USDA For. Serv. Res. Pap. PNW-252. 13 p.

Cooper, S.V., K.E. Neiman, R. Steele, and D.W. Roberts. 1991. Forest habitat types of northern Idaho: a second approximation. USDA For. Serv. Gen. Tech. Rep. INT-236. 143 p.

Corona, P., R. Scotti, and N. Tarchiani. 1998. Relationship between environmental factors and site index in Douglas-fir plantations in central Italy. For. Ecol. Manage. 110:195-207.

Curt, T. 1999. Predicting yield of Norway spruce and Douglas-fir using a morphopedological approach in the granitic landscapes of French Massif Central. Can. J. Soil Sci. 79:491-500.

Curt, T., M. Bouchaud, and G. Agrech. 2001. Predicting site index of Douglas-fir plantations from ecological variables in the Massif Central area of France. For. Ecol. Manage. 149:61-74.

Dahlgren, R., S. Shoji, and M. Nanzyo. 1993. Mineralogical characteristics of volcanic ash soils. *In* S. Shoji. et al. (ed.). Volcanic ash soils – Genesis, properties, and utilization. Elsevier, Amsterdam. pp. 101-144.

Fotheringham, A.S., C. Brunsdon, and M. Charlton. 2002. Geographically weighted regression: The analysis of spatially varying relationships. John Wiley and Sons, New York. 265 p.

Garrison-Johnston, M.T., R. Lewis, and T. Frost. 2003. Geologic controls on tree nutrition and forest health in the Inland Northwest. Abstracts with Programs – Geological Society of America. 35(6):433.

Graney, D.L. 1977. Site index predictions for red oaks and white oak in the Boston mountains of Arkansas. USDA For. Serv. Res. Pap. SO-139. 9 p.

Green, R.N., P.L. Marshall, and K. Klinka. 1989. Estimating site index of Douglas-fir (*Pseudotsuga menziesii* [Mirb.] Franko) from ecological variables in southwestern British Columbia. For. Sci. 35:50-63.

GWR. 2005. Geographically weighted regression software 3.0. National Centre for Geocomputation. National University of Ireland. Maynooth, Ireland.

Hope, A. 1968. A simplified Monte Carlo significance test procedure. J. Royal Statist. Soc. Ser. B. 30:582-598.

Idaho State Climate Services. 2000. Digital precipitation for Idaho: Average, monthly, and annual (1961-1990). Idaho State Climate Services. Moscow, ID.

Kabzems, R.D., and K. Klinka. 1987. Initial quantitative characterization of soil nutrient regimes. II. Relationships among soils, vegetation, and site index. Can. J. For. Res. 17:1565-1571.

Kayahara, G.J., K. Klinka, and P.L. Marshall. 1998. Testing site index–site-factor relationships for predicting *Pinus contorta* and *Picea engelmannii* x *P. glauca* productivity in central British Columbia, Canada. For. Ecol. Manage. 110:141-150.

Kimsey, M.J., B. Gardner, and A. Busacca. 2006. *In Press.* Ecological and topographic features of volcanic ash-influenced forest soils. *In* D. Page-Dumroese et al. (ed.). Volcanic-ash-derived forest soils of the Inland Northwest: Properties and implications for management and restoration. USDA For. Serv. Proc. RMRS-XXX.

McDaniel, P.A., R.W. Gabehart, A.L. Falen, J.E. Hammel, and R.J. Reuter. 2001. Perched water tables on argixeroll and fragixeralf hillslopes. Soil Sci. Soc. Am. J. 65:805-810.

McDaniel, P.A., M.A. Wilson, R. Burt, D. Lammers, T.D. Thorson, C.L. McGrath, and N. Peterson. 2005. Andic soils of the Inland Pacific Northwest, USA: Properties and ecological significance. Soil Sci. 170:300-311.

McKenney, D.W., and J.H. Pedlar. 2003. Spatial models of site index based on climate and soil properties for two boreal tree species in Ontario, Canada. For. Ecol. Manage. 175:497-507.

McLeod, S.D., and S.W. Running. 1988. Comparing site quality indices and productivity in ponderosa pine stands of western Montana. Can. J. For. Res. 18:346-352.

Monserud, R.A. 1984. Height growth and site index curves for inland Douglas-fir based on stem analysis data and forest habitat type. For. Sci. 30:943-965.

Monserud, R.A. 1985. Comparison of Douglas-fir site index and height growth curves in the Northwest. Can. J. For. Res. 15:673-679.

Monserud, R.A., U. Moody, and D. Breuer. 1990. A soil-site study for inland Douglas-fir. Can. J. For. Res. 20:686-695.

Monserud, R.A., and G.E. Rehfeldt. 1990. Genetic and environmental components of variation of site index in Douglas-fir. For. Sci. 36:1-9.

Myers, R.H. 1990. Classical and modern regression with applications. Ed. 2. Duxbury, Pacific Grove, CA. 488 p.

Reiche, P. 1943. Graphic representation of chemical weathering. J. Sed. Petrol. 13(2):58-68.

Rockefeller, S.L., P.A. McDaniel, and A.L. Falen. 2004. Perched water table responses to forest clearing in northern Idaho. Soil Sci. Soc. Am. J. 68:168-174.

Rodríquez, F. S., R.R. Soalleiro, E. Espaňol, C.A. López, A. Merino. 2002. Influence of edaphic factors and tree nutritive status on the productivity of *Pinus radiata* D. Don plantations in northwestern Spain. Forest Ecol. Manage. 171:181-189.

Roise, J.P., and D.R. Betters. 1981. An aspect transformation with regard to elevation for site productivity models. For. Sci. 27:483-486.

SAS Institute, Inc. 1990. SAS/STAT User's guide. SAS Institute Inc., Cary, NC. 1686 p.

Schoenholtz, S. H., H. van Miegroet, and J.A. Burger. 2000. A review of chemical and physical properties as indictors of forest soil quality: challenges and opportunities. Forest Ecol. Manage. 138:335-356.

Spurr, S.H., and B.V. Barnes. 1980. Forest ecology. Ed. 3. Wiley, New York. 687 p.

Stage, A.R. 1976. An expression for the effect of aspect, slope, and habitat type on tree growth. For. Sci. 22:457-460.

Steele, R., R.D. Pfister, R.A. Ryker, and J.A. Kittams. 1981. Forest habitat types of central Idaho. USDA For. Serv. Gen. Tech. Rep. INT-114. 137 p.

Stendahl, J., S. Snäll, M.T. Olsson, and P. Holmgren. 2002. Influence of soil mineralogy and chemistry on site quality within geological regions in Sweden. Forest Ecol. Manage. 170:75-88.

Uzoh, F.C.C. 2001. A height increment equation for young ponderosa pine plantations using precipitation and soil factors. For. Ecol. Manage. 142:193-203.

Vander Ploeg, J.L., and J.A. Moore. 1989. Comparison and development of height growth and site index curves for Douglas-fir in the Inland Northwest. West. J. Appl. For. 4(3):85-88.

Wang, Y., F. Raulier, and C.H. Ung. 2005. Evaluation of spatial predictions of site index obtained by parametric and nonparametric methods – A case study of lodgepole pine productivity. For. Ecol. Manage. 214:201-211.

Wang, G.G, and K. Klinka. 1996. Use of synoptic variables in predicting white spruce site index. For. Ecol. Manage. 80:95-105.